Earth tides and ocean tides

Because so obvious + important to seafaring nations, ocean tides observed far back into history.
Before Newton many colorful "explanations".

Ch. IV of The Tides (1898) by Sir G. Darwin, charming Victorian book for lay audience:
p. 79, from Koran: displacement by foot of an angel
p. 76, "Chinese writers have suggested... that H_2O is the blood of the ⊕ and that the tides are the beating of its pulse".

Many early observers ~~[illegible]~~ noticed correlation with ☾, esp. spring and neap tides with full and new and half ☾, respectively.
Early explanations of this: heat from ☉ dries up oceans, moisture from ☾ etc.

Greeks and Romans had little cause to ponder the tides as they are very small everywhere in the Mediterranean.

1687 Newton's Principia : first correct discussion in terms of gravitational attraction of ☾, ☉ on oceans. His a static theory. Concept of equilibrium tide still plays important role in theory.

Next important development 1774 Laplace's Mechanique Celeste : realized that problem of ocean tides a dynamical one. Can think of tide as a deep water wave

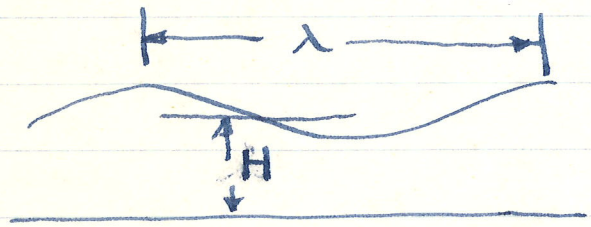

$\lambda \gg h$, thus phase velocity $c = \sqrt{gH}$

$H \sim 5$ km, deep oceans

$c \sim (10^3 \cdot 5 \cdot 10^5)^{1/2} \sim 2 \cdot 10^4 - 3 \cdot 10^4$ cm/s

$\sim 700 - 1000$ km/hr

Across an ocean basin + return in a time of order 12 hr = period of forcing ⟹ resonance effects ; this invalidates a quasi-static theory.

<u>Analogy</u>: a <u>pendulum</u> (or any other simple harmonic oscillator)

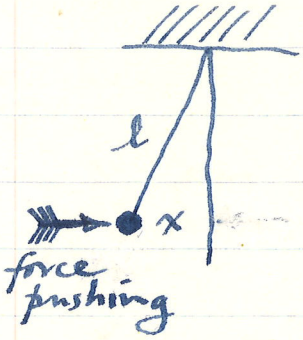

period $T = 2\pi\sqrt{l/g}$, time to complete one cycle.

Say one pushes laterally with a force which varies sinusoidally with a period $T_{force} \gg T$. Then response will be quasi-static or <u>equilibrium</u>, i.e. all forces will be in <u>static</u> balance at all times, <u>acceleration</u> of mass negligible. But if $T_{force} \sim T$ <u>resonance</u> effects can occur, response more complicated, must solve eqns of motion with <u>acceleration</u> term $\ddot{x}$

Laplace derived eqns of motion for tides on a sphere including <u>acceleration</u> terms and rotation. Only in last few years have computers been adequate to solve <u>L.T.E.</u> numerically for realistic oceanic depths $h(\theta, \phi)$ on $\oplus$ surface.

Lord Kelvin designed first self-recording <u>tide</u> <u>gauge</u> ~ 1860's, previously measured on <u>tide</u> <u>poles</u> (meter sticks read by eye), difficulty with waves, averaged by eye.

Kelvin's gauge damped out the waves so could record mechanically.

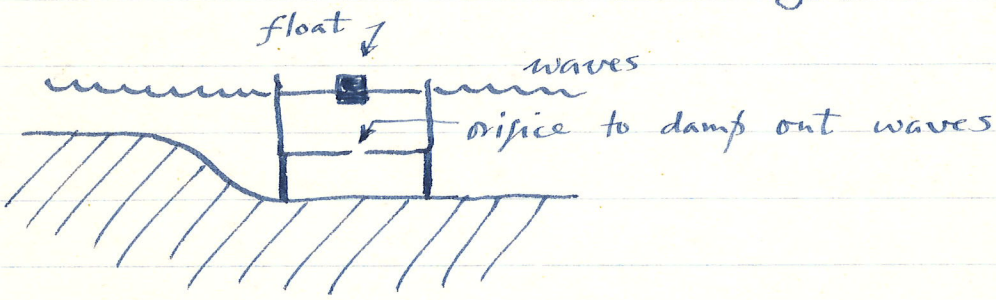

Study of tides long hindered by inability to make measurements in <u>deep</u> oceans, only on coasts + scattered islands.
Two techniques now for measuring deep-sea tides:

1. pressure gauges on bottom: tides are deep water waves so $\Delta p = \rho g h$ <u>on bottom</u> (h = height of tide); technology: free-fall retrievable capsules.

2. radar altimetry from satellites, if can measure ζ to $\pm$ few cm, can measure variations, this method holds much promise, few concrete results to date.

Kelvin 1876 also first to point out that tidal forces would cause deformations of <u>solid</u> ⊕ as well, since ⊕ not completely rigid.

Surface of solid ⊕ raised by 10–20 cm, tidal strains $\Delta l / l \sim 10^{-7}$ or 10^{-8} measured with <u>strain meters</u>.

$\Delta l / l \sim 10^{-7}$ to 10^{-8}

Two types in common use:

1. Benioff <u>quartz</u> rod, low coeff. of thermal expansion, still must site in mine or tunnel, typically uses capacitive transducer

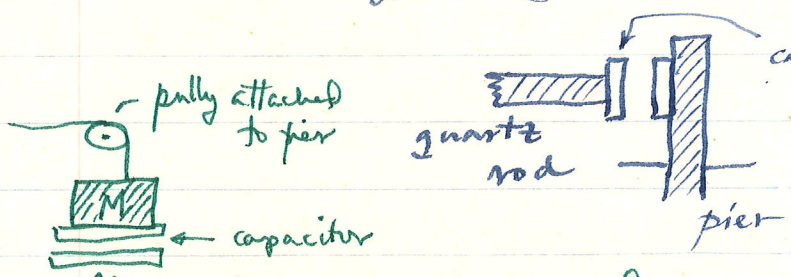

measure $C(t)$ by measuring $\omega = \sqrt{LC}$ of a tuned circuit

Alternative: a stretched Invar wire

typically $l \sim 50 - 100$ m, the longer the better to average out local "geology". If $l = 100$ m

then $\Delta l \sim 0.01$ to 0.001 mm.

2. <u>laser interferometer</u>: stable and precise, but more expensive, not too many $\exists$. Might look like this:

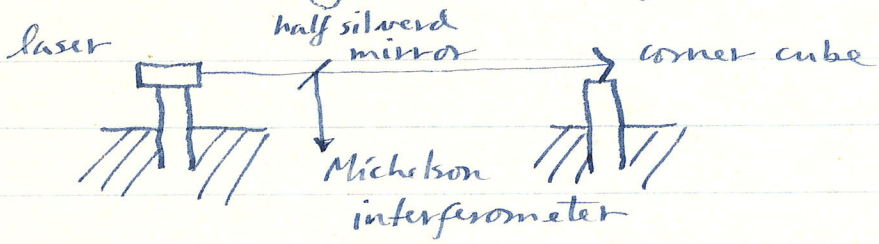

measures strain in fringes, or wavelengths of He-Ne light. Two problems: changes in refractive index of air, must evacuate pipe, expensive, pumps, etc. esp. for a ~ 1 km instrument. under development: 3 "color" system measure temp, humidity of air + $\Delta l / l$ simultaneously. Second problem: He-Ne laser not sufficiently <u>stable</u>, must be stabilized, e.g. with <u>methane</u> absorption servo cell.

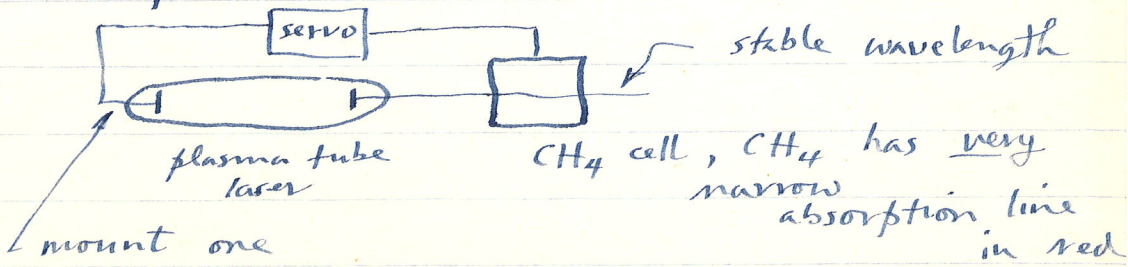

There are also tidal gravity fluctuations $\Delta g/g \sim 10^{-7}$ to 10^{-8} $\sim$ 0.1 to 0.01 mgal (recall $g \sim 980$ gal $\equiv$ cm/s^2)

Measured with long-period seismometers Essentially mass on a spring. Three types in use:

1. Lacoste:

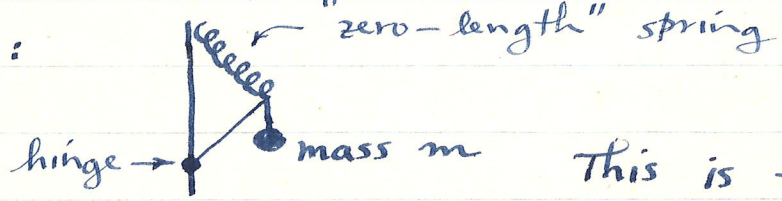

This is the basic geometry.

For use in IDA network, electrostatic capacitive feedback has been added as a way to measure deflection of mass; general idea:

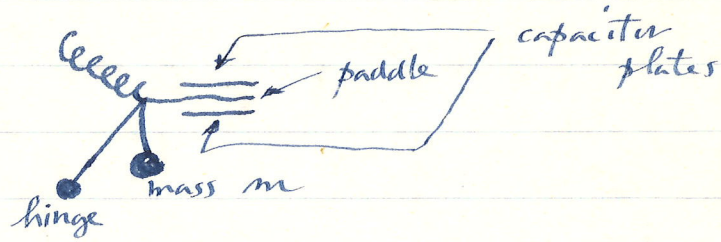

apply a voltage $V(t)$ to keep paddle centered between two plates. Actual "signal" is servo voltage required to do this.

2. Block-Moore: capacitive feedback system first developed for use with this instrument, only the "spring" is different.

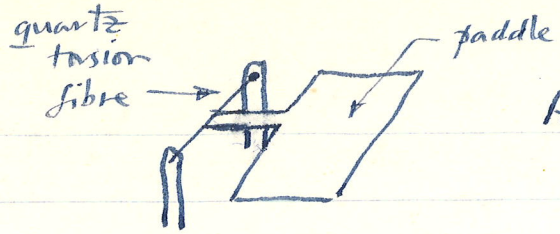

Here the paddle plays the role of the mass too

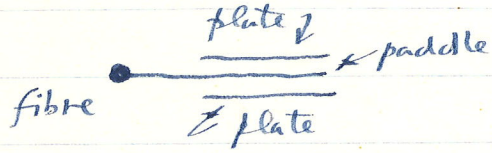

3. <u>superconducting</u> : the ultimate in stability, sensitivity and $. A superconducting sphere about 2 cm in diameter is levitated in a magnetic field. Liquid He temps. guarantee a very low Brownian noise level. Electrostatic feedback is again used to maintain the posn. of the ball when g changes.

There are also tiltmeters that measure tilt ≡ horizontal acceleration, e.g. liquid level tiltmeters (Michelson–Gale)

Earth tides much more nearly <u>equilibrium</u> than ocean tides, fund. period of solid ⊕ $_0S_2$ mode ~ 54 min. period ≪ 12 hr. semi-diurnal tide. Time for P wave to go thru center of ⊕ and return ~ 40 min.

⊕ tide measurements are however contaminated by <u>ocean</u> <u>loading</u>.

☾

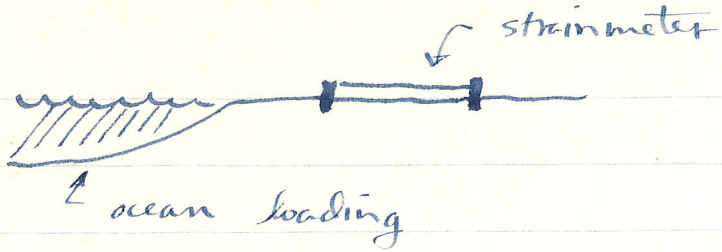

causes extra strains, especially near coasts.

This makes it very difficult to determine some things we'd like to know, e.g. fraction of tidal energy dissipated by bodily friction.

Why are there 2 tides / day instead of one? Grav. attraction of ☾ at pts. on ⊕ surface (i.e. on ocean H_2O particles) varies from place to place.
Neglect ☉ for moment.

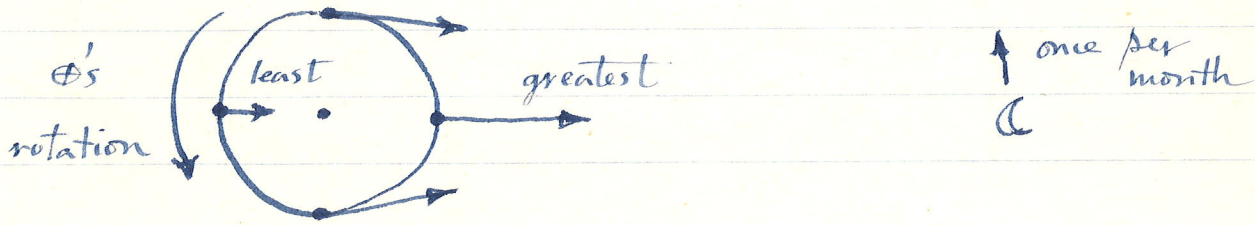

Looks like should only be 1 tide / day as ⊕ rotates under <u>tidal</u> <u>bulge</u> (by day we mean <u>lunar</u> day)

But actually ⊕ and ☾ <u>revolve</u> <u>mutually</u> about their common c.o.m.

Every pt. on ⊕ experiences the <u>same</u> <u>orbital acceleration</u>. This point obfuscated in many if not most elementary discussions like this one.

Where is c.o.m.? ⊕☾ – distance ~ 60 ⊕ radii, $M_☾ / M_⊕ = 1/81.3$.

Thus:

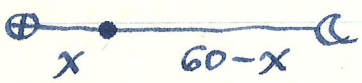

$$81.3x = 60 - x$$
$$x = 60/82.3$$
$$\approx 3/4$$

⊕☾ c.o.m. about 3/4 of way out to ⊕ surface.

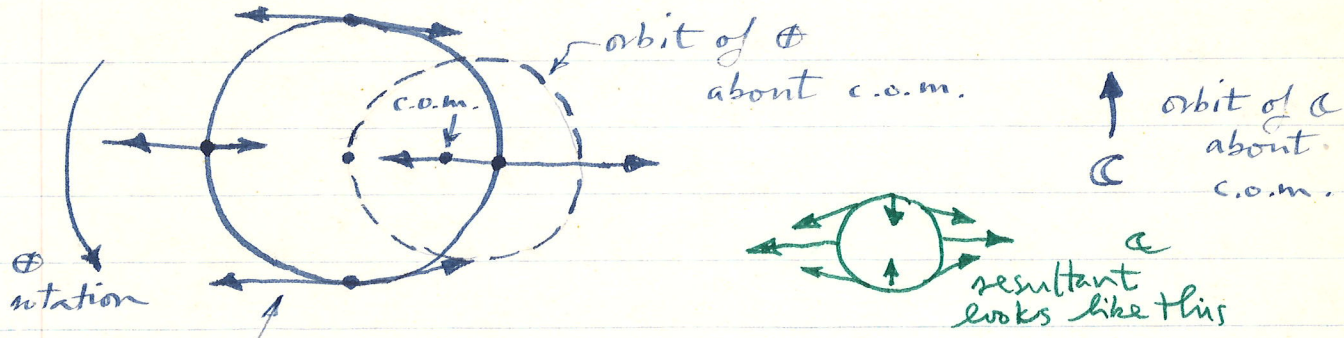

orbital acceleration; every ← arrow of <u>same</u> <u>length</u> (as well see in derivation below)

motion of every pt. on ⊕ is superposition of orbital accel. of c.o.m. ← is <u>not</u> a <u>centripetal</u> acceleration + ⊕'s rotation about c.o.m. but an <u>orbital</u> acceleration

it's the <u>same</u> at every pt. on ⊕ because every pt. experiences the same orbital motion, hence same $\frac{d^2}{dt^2}$ motion

<u>Resultant</u> looks like: tries to squeeze ⊕ into an egg shape

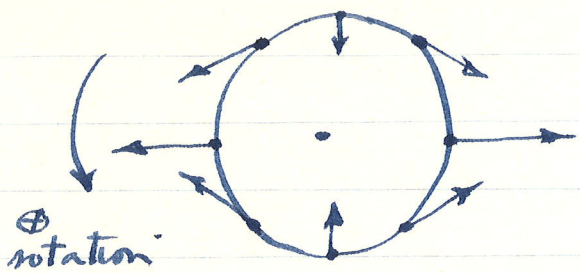

☾
moon

If no ☉ and response equilibrium would be 2 tides / lunar day. The ☉ causes an additional spring-neap variation.

The tidal potential

Assumptions: all of ☉, ☾, ⊕ spherically symmetric, thus ☉, ☾ may be treated as distant pt. masses.
Ellipticity of ⊕ would change ht. of theoretical tide by 1/300 which we neglect.

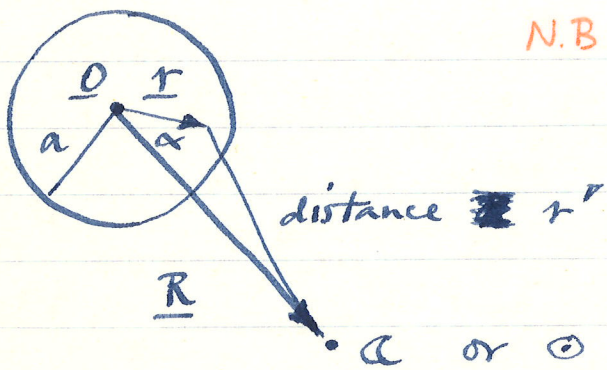

N.B. α is local zenith angle of ☾

O: c.o.m. of ⊕ (and origin)
r: pt. of obs. of tide, not necessarily at ⊕ surface
r′: dist. from ☾ or ☉ to obs. pt.
R: posn. of ☾ or ☉
a: radius of ⊕

Treat ☾, ☉ separately by principle of superposition.
We consider, e.g., the ☾.

1. net grav. force of ☾ on (all of) ⊕ is $\underline{f} = GM_{\oplus} M_{☾} \hat{R} / R^2$.

2. acceleration of $\oplus$ in its orbit due to this force

$$\underline{A} = \underline{f} / M_{\oplus} = G M_{☾} \hat{R} / R^2.$$

N.B. independent of $\underline{r}$ = obs. pt (all ← arrows same)

3. grav. pot. of ☾ at pt. $\underline{r}$

$$\phi_{☾}(\underline{r}) = -\frac{G M_{☾}}{r'}$$

$$= -\frac{G M_{☾}}{R} \sum_{l=0}^{\infty} \left(\frac{r}{R}\right)^{l} P_l(\cos\alpha)$$

$$\left(\cos\alpha = \hat{r} \cdot \hat{R}\right)$$

4. we view tides in an <u>accelerated</u> reference frame, namely on the $\oplus$. <u>D'Alembert's principle</u>: represent this acceleration by a fictitious force. The resultant is the <u>tidal force</u>. Net tidal force at $\underline{r}$ is:

$$-\nabla\phi_{☾}(\underline{r}) - \underline{A}$$

variable ↗ ↑ constant ← vector

But $-\nabla\phi_{☾}(\underline{r}) - \underline{A}$

$$= -\nabla\left[\phi_{☾}(\underline{r}) + \underline{r} \cdot \underline{A}\right]$$

5. $$\phi_{☾}(\underline{r}) + \underline{r}\cdot\underline{A} = -\frac{GM_{☾}}{R}\left[1 + \frac{r}{R}\cos\alpha + \sum_{l=2}^{\infty}\left(\frac{r}{R}\right)^{l} P_l(\cos\alpha)\right] + \frac{GM_{☾}}{R}\frac{r}{R}\cos\alpha$$

$$= \underbrace{-\frac{GM_{☾}}{R}}_{\text{const}} - \frac{GM_{☾}}{R}\sum_{l=2}^{\infty}\left(\frac{r}{R}\right)^{l} P_l(\cos\alpha)$$

The <u>const</u> term is the pot. of ☾ at c.o.m. of ⊕; when take ∇ gives rise to no force ∴ is of no interest (the usual arbitrary const. in potential theory).

Note $l = 1$ term has been <u>cancelled</u> by <u>A</u> term. This term gives rise to a <u>uniform</u> force throughout ⊕, viz. $GM_{☾}\hat{R}/R^2$. But this is precisely the force which keeps ⊕ accelerating in its Keplerian orbit.

<u>Tidal</u> forces, the <u>resultant</u>, on contrary due to small variations throughout ⊕ of grav. force / mass exerted by ☾.

c. Let $$V_{☾}(\underline{r}) = -\frac{GM_{☾}}{R}\sum_{l=2}^{\infty}\left(\frac{r}{R}\right)^{l} P_l(\cos\alpha)$$

This called the (lunar) <u>tidal potential</u>.

A note on the derivation of the tidal potential:

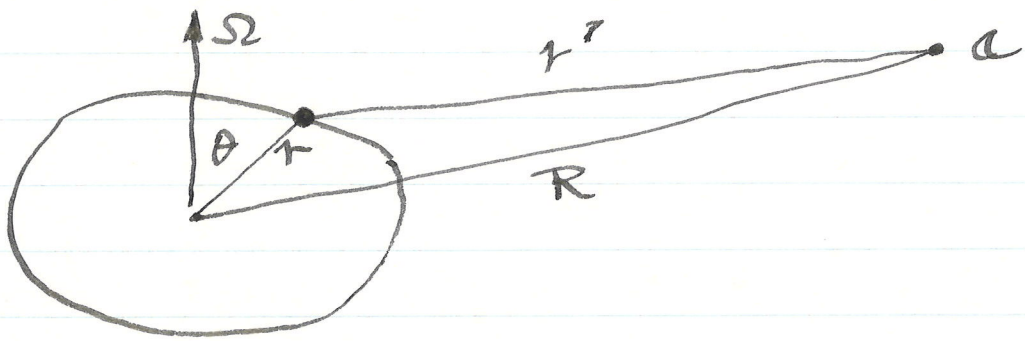

The total grav. pot. at the point • is:

$$V_{\oplus}(\text{due to } \oplus) - \frac{GM_{☾}}{r'(t)}$$

Due to its motion relative to inertial space, observer at • also "feels" fictitious forces. The motion at any pt. • can always be regarded as the superposition of motion of c.o.m. (the orbital motion of ⊕) + motion w.r.t. c.o.m. (the ⊕'s rotation $\underline{\Omega}$).

The total fictitious force is $-\nabla$ of:

$$\underbrace{-\tfrac{1}{2}\Omega^2 r^2 \sin^2\theta}_{\text{due to rotation}} + \underbrace{\underline{r}\cdot\underline{A}}_{\text{due to orbital acceleration of c.o.m.}}$$

But $-\nabla\left[V_{\oplus} - \frac{1}{2}\Omega^2 r^2 \sin^2\theta\right] = -\nabla U_{\text{geopot.}} = \underline{g}$ $\boxed{\text{no change with } t \text{ on a rigid } \oplus}$

$\underline{f}(\underline{r}) = -\nabla V(\underline{r})$ called <u>tidal force</u>.
Pictorial repr. of $\underline{f}(\underline{r})$ on surface $r=a$ of $\oplus$ is:

Another pt. of view: let $\underline{f}_{tot}(\underline{r}) \equiv$ force exerted by moon on a unit mass at $\underline{r}$. Then $\underline{f}(\underline{r}) =$ tidal force $= \underline{f}_{tot}(\underline{r}) - \underline{f}_{tot}(\underline{0})$. Tidal force is diff. in force at $\underline{r}$ from force at origin $\equiv$ c.o.m. $\oplus$. (Including the fictitious force due to the orbital acceleration)

Examine <u>relative</u> magnitude of terms in sum (at $\oplus$ surface $r=a$):

$$\underbrace{\left(\frac{a}{R}\right)^2 P_2(\cos\alpha)}_{\text{order } 1} + \underbrace{\left(\frac{a}{R}\right)^3 P_3(\cos\alpha)}_{\text{order } 1} + \cdots$$

relative order $\left(\frac{a}{R}\right)$

for ☾: $\frac{a}{R} \sim 1/60$
for ☉: $\frac{a}{R} \sim 1/23{,}000$

For ☉ can <u>certainly</u> neglect all but $l=2$. For ☾, terms $l>2$ lead to tides $\sim 1/60$ of $l=2$ tides, can be observed as they occur 3 (and 4, etc.) times per day, but

for moment we neglect them. Then

$$\boxed{V_{☾}(\underline{r}) = -\frac{GM_{☾}}{R}\left(\frac{r}{R}\right)^2\left(\frac{3}{2}\cos^2\alpha - \frac{1}{2}\right)}$$

<u>lunar</u> <u>tidal</u> <u>potential</u>, similar for ☉

What is <u>relative</u> effect of ☾ and ☉ in raising tides on ⊕?

$$V_{☾} \sim \frac{M_{☾}}{R_{☾}^3}, \quad V_{☉} \sim \frac{M_{☉}}{R_{☉}^3} \quad \text{so}$$

$$☾/☉ \sim \frac{M_{☾}/R_{☾}^3}{M_{☉}/R_{☉}^3} = \frac{\bar{\rho}_{☾}}{\bar{\rho}_{☉}}\left(\frac{a_{☾}/R_{☾}}{a_{☉}/R_{☉}}\right)^3$$

Now a/R is the <u>visible half-aperture</u> in sky.

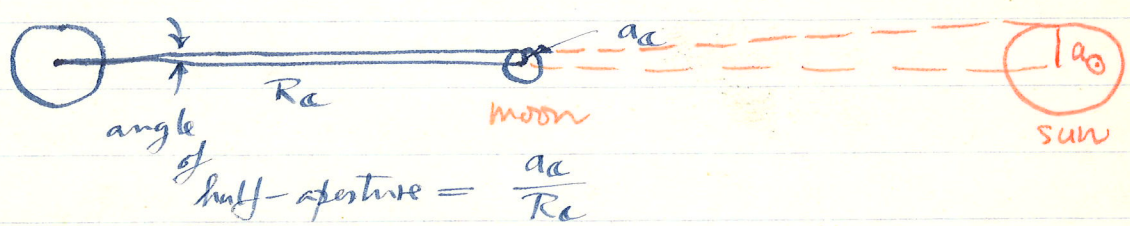

The visible apertures of ☾ and ☉ are very nearly equal (we have eclipses). Thus the effect ~ <u>ratio</u> of <u>densities</u>!

$$\bar{\rho}_{☾} \sim 3.3$$
$$\bar{\rho}_{☉} \sim 1.4$$

$$\frac{☾}{☉} \sim \frac{3.3}{1.4} \sim \frac{1}{0.46}$$

$$\boxed{☾ \text{ effect a little more than twice } ☉}$$

Tidal force of ☾ acting up will cause a 90 kg person to lose 10 mg weight (1 part in $\sim 10^7$ $\delta g/g$ change). This ~ weight one drop of sweat.

Question: then how come tides are are as large as they are?
Answer: tides are result of tangential forces + cons. of mass (no resistance to tang. motion)

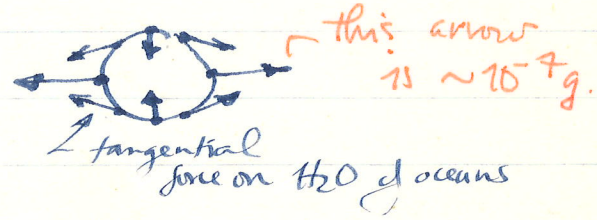

One last question: what is relative effect of ☉ and ⊕ on lunar tides (on ☾)?

Solar tides on ☾ ~ solar tides on ⊕.
Terr. tides on ☾:

$$⊕/☉ \sim \frac{M_⊕/R_⊕^3}{M_☉/R_☉^3} \sim \frac{200}{1}$$

Tides on ☾ dominated by ⊕: ~200 times

bigger than tides on ⊕.

Note: ☾ always keeps same face toward ⊕ (a result of (past) tidal friction, as we shall see). Thus:

monthly = dominant tidal period on ☾ due to eccentricity of orbit

The majority of moonquakes (much smaller in energy release or magnitude than large earthquakes) appear to be tidally triggered

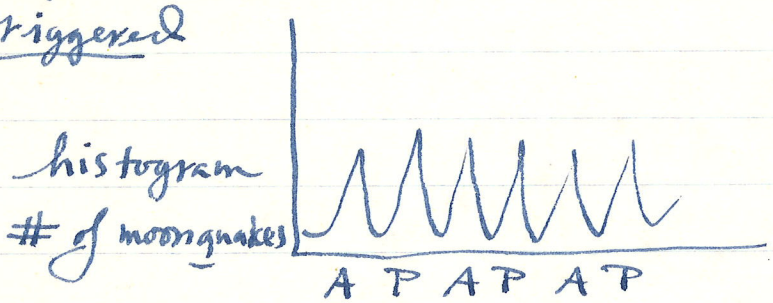

A = apogee
P = perigee

No (or only occasional weak) evidence of tidal triggering of quakes on ⊕. Two reasons for difference:

1. difference in ⊕ ☾ interior properties: ☾ smaller, thicker lithosphere, colder, ⊕ convecting, dominated by tectonic strains.
2. tides on ☾ 200 times bigger than tides on ⊕.

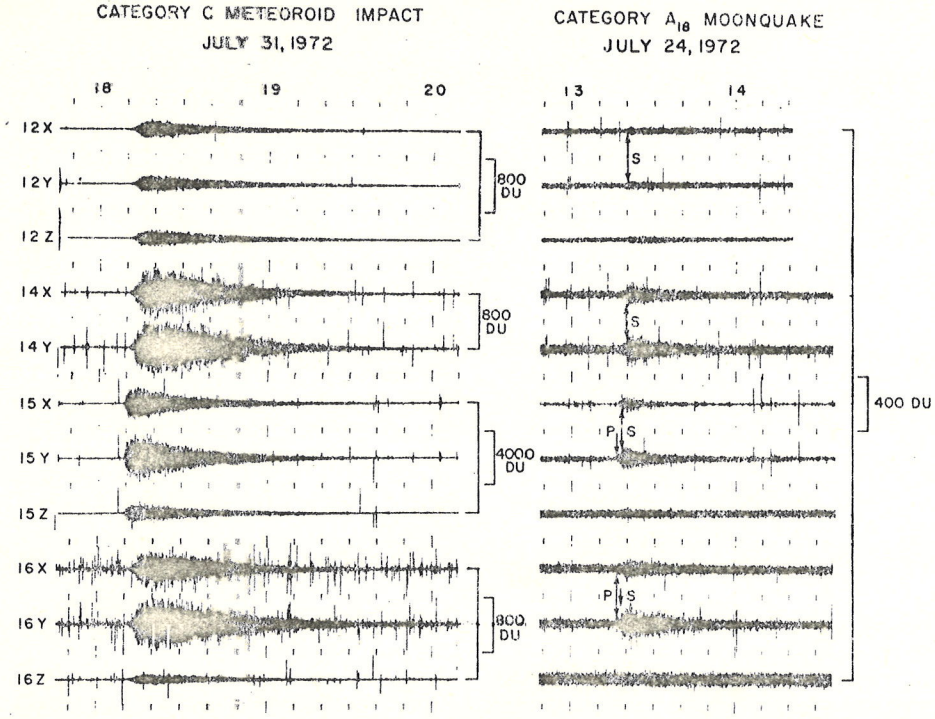

Fig. 4. Compressed time-scale records of LP components for two natural seismic events recorded at four seismic stations; X and Y refer to the horizontal component seismometers; Z refers to the vertical component seismometers. Each successive trace deflection of a LP compressed time scale record represents the sum of the absolute values of the differences between 40 successive data samples during consecutive, nonoverlapping 6-s time intervals. Successive deflections are plotted on opposite sides of the zero base line. The relative amplitudes of the signals are indicated by the brackets following each record. Tick marks are 10 min apart, and hours are labeled. The category A_{18} moonquake zone is located at the eastern border of Mare Serenitatis (see Table 3). For category A moonquakes, the direct shear wave *S* is prominent on seismograms from the horizontal seismometers. The direct compressional wave *P* is observed on seismograms of the largest category A moonquakes. The category C meteoroid impacted roughly 500 km north of station 15. The onsets of the direct compressional and shear waves can rarely be identified on LP seismograms of category C events.

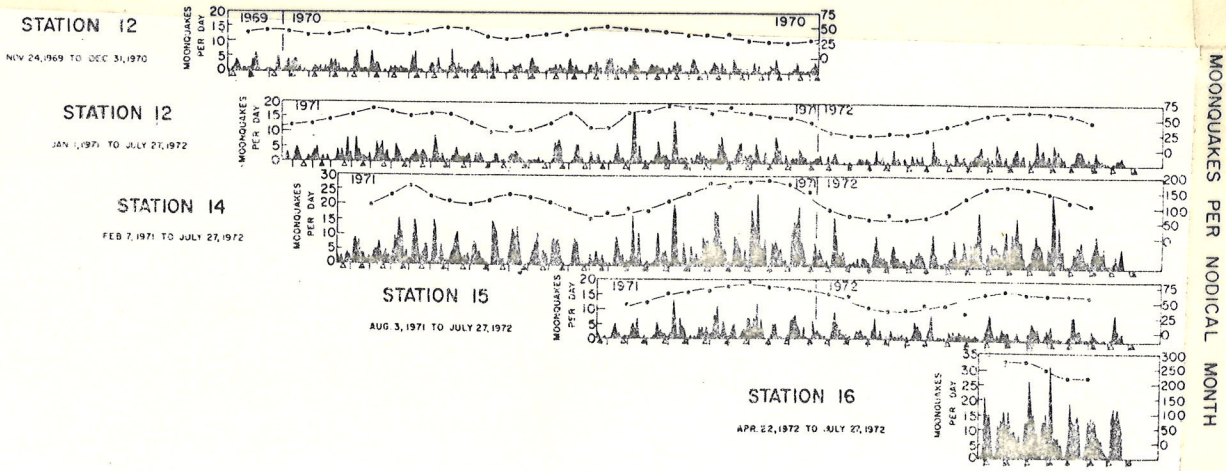

Fig. 10. Category A and B seismic activity detected by the Apollo seismic network during the period November 24, 1969, to July 27, 1972. The number of category A and B events detected per day at each station is plotted as a function of time. The time interval covered by each of the stations is given in the figure. The solid triangles indicate times of perigee, and the open triangles indicate times of apogee. The vertical lines below each figure indicate the times of the maximum latitudinal librations. The maximum longitudinal librations occur at times intermediate to apogee and perigee. In general, two peaks in seismic activity are observed at all stations each nodical month at times intermediate to the maximum latitudinal librations. The peaks appear to show no fixed time relationship to apogee and perigee. The dashed curves in each figure represent the number of events detected per nodical month. Points are plotted at times of successive maximum latitudinal librations and each point represents the number of events detected in the preceding and following half-nodical month intervals. A long-period variation (about 206 days) in the number of events detected per month is observed at stations 12, 14, and 15 during 1971 and 1972, but not at station 12 during 1969 and 1970.

The equilibrium tide (Newton)

Consider spherical ⊕ with no ☾ or ☉ in sky. Equipotential surfaces are spherical. Consider the surface $r = a$ = radius of ⊕.

Let $\phi_0(\underline{r})$ be grav. pot. of ⊕. On $r = a$, $\phi_0(\underline{r}) = \phi_0 = -GM_\oplus/a$ = const.

Let $\underline{g}(\underline{r}) = -\nabla\phi_0(\underline{r})$ grav. acceleration and let $g \equiv |\underline{g}(\underline{r})|$ on $r = a$ so that $\underline{g}(\underline{r}) = -g\hat{r}$ on $r = a$. Then $g = GM_\oplus/a^2$.

Now consider ⊕ + tide-generating bodies. What will be new, deformed shape of surface with pot. = const. = ϕ_0?

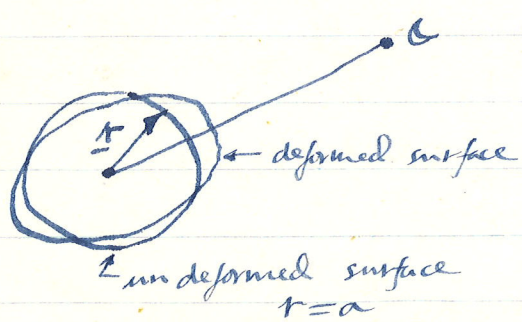

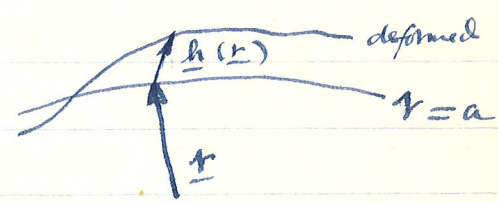

Say pt. $\underline{r}$ moves to $\underline{r} + \underline{h}(\underline{r})$. Let $\phi(\underline{r})$ = total pot. including tidal pot. at an arbitrary pt. $\underline{r}$.

$$\phi(\underline{r}) \equiv \phi_0(\underline{r}) + V(\underline{r})$$

On the displaced surface:

$$\phi(\underline{r}+\underline{h}) = \phi_0(\underline{r}+\underline{h}) + V(\underline{r}+\underline{h})$$
$$= \phi_0(\underline{r}) + \underline{h}\cdot\nabla\phi_0(\underline{r}) + \cdots$$
$$+ V(\underline{r}) + \cdots \quad \text{where}$$

$\cdots$ is $O(|\underline{h}|^2)$ which we neglect.

$$= \phi_0(\underline{r}) - \underline{g}\cdot\underline{h} + V(\underline{r})$$

$$= \phi_0(\underline{r}) + g h_r(\underline{r}) + V(\underline{r})$$

now let us denote $h_r \equiv \hat{r}\cdot\underline{h}$ by h

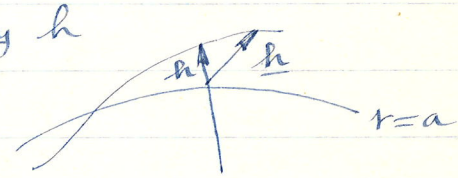

h is the <u>radial displacement</u> (up and down) of equipot. surface.

$$\phi(\underline{r}+h) = \phi_0(\underline{r}) + g\,h(\underline{r}) + V(\underline{r}) + \cdots$$

this is $\phi_0 =$ const. (initial pot. on $r = a$)

we want this to be ϕ_0 too (new total pot. on displaced surface).

Thus on surface of $\oplus$, $r = a$, displacement of equipot. surface is given by

$$h(\underline{r}) = -\frac{1}{g} V(\underline{r})$$

called the equilibrium tide

Note: this same argument we used before to find geoid signal N in terms of anomalous potential V over a mid-ocean ridge.

h, the equilibrium tide: if $\oplus$ were rigid + covered by thin oceans and if tidal potential V changed very slowly so ocean always had time to respond, then $\underline{\oplus}$ would always be equipotential and the tide would be h. Real tides are dynamical because time scale for changes of $V \approx$ natural resonant periods of ocean basins.

Equilibrium tide still a useful concept: can think of as input to system.

$$h = -\frac{1}{g} V \quad , \quad g = \frac{GM_\oplus}{a^2}$$

$$V_a = -\frac{GM_a}{R}\left(\frac{a}{R}\right)^2 P_2(\cos\alpha)$$

Thus $$h_{☾} = a \frac{M_{☾}}{M_{\oplus}} \left(\frac{a}{R}\right)^3 P_2(\cos\alpha)$$

$$\boxed{\text{Let } \bar{R} \equiv \underline{\text{mean}}\ \oplus☾ \text{ distance, a fixed number} \sim 60\ \oplus \text{ radii.}}$$

Then

$$\boxed{\begin{aligned} h_{☾}(\underline{r}, t) &= K_{☾} \left(\frac{\bar{R}}{R}\right)^3 P_2(\cos\alpha) \\ \text{where } K_{☾} &\equiv a \underbrace{\frac{M_{☾}}{M_{\oplus}}}_{1/81.3} \underbrace{\left(\frac{a}{\bar{R}}\right)^3}_{(1/60)^3} \\ &= 35.785 \text{ cm} \end{aligned}}$$

Likewise

$$h_{\odot}(\underline{r}, t) = \text{same with } K_{\odot}$$

$$\boxed{K_{\odot} = 16.427 \text{ cm} \sim \tfrac{1}{2} K_{☾}}$$

recall: α is local zenith angle of ☾

Note $(\bar{R}/R)^3$ and $P_2(\cos\alpha)$ vary with <u>time</u>.

$(\bar{R}/R)^3$: changing distance with time

$P_2(\cos\alpha)$: changing direction with time.

Both factors are of order 1, so $K_{☾}$ and

$K_\odot$ are typical equil. tide heights. Note $K_\odot \sim \frac{1}{2} K_☾$ as noted already.

Recall that $\alpha(t)$ is angle between ☾ or ⊙ and local zenith. Consider a standard (geocentric) coord system:

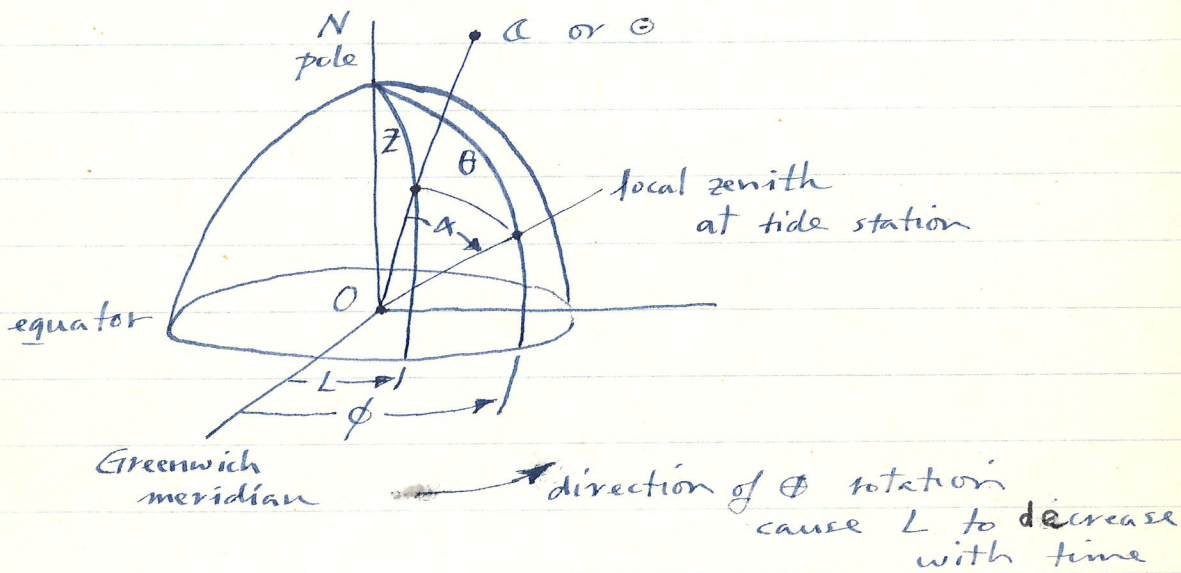

θ, ϕ: colatitude, longitude at station or obs. pt.

$Z(t)$, $L(t)$: colatitude, longitude of ☾ or ⊙

By spherical trigonometry, or more elegantly by the spherical harmonic addition theorem can be shown that:

$$P_2(\cos\alpha) \equiv \frac{3}{2}\cos^2\alpha - \frac{1}{2}$$

$$= \left(\frac{3}{2}\cos^2\theta - \frac{1}{2}\right)\left(\frac{3}{2}\cos^2 Z - \frac{1}{2}\right)$$
$$+ \frac{3}{4}\sin 2\theta \sin 2Z \cos(L-\phi)$$
$$+ \frac{3}{4}\sin^2\theta \sin^2 Z \cos 2(L-\phi)$$

This the term involving $\alpha(t)$ written in terms of colat. and long. of ☾ or ☉ and station. Can then write equil. tide in form:

$$\boxed{\begin{aligned} h_{☾}(\theta,\phi,t) = {} & K_{☾}\left[\tfrac{3}{2}\cos^2\theta - \tfrac{1}{2}\right]\left[\left(\frac{\bar{R}}{R}\right)^3\left(\tfrac{3}{2}\cos^2 Z - \tfrac{1}{2}\right)\right] \\ & + K_{☾}\left[\sin 2\theta\right]\left[\tfrac{3}{4}\left(\frac{\bar{R}}{R}\right)^3 \sin 2Z \cos(L-\phi)\right] \\ & + K_{☾}\left[\sin^2\theta\right]\left[\tfrac{3}{4}\left(\frac{\bar{R}}{R}\right)^3 \sin^2 Z \cos 2(L-\phi)\right] \end{aligned}}$$

equilibrium tide at a point θ, ϕ on ⊕'s surface as function of time (similarly for $h_{☉}$)

Sum of 3 terms, each of form

$$\boxed{K_{☾}\left[\text{shape of ⊕'s surface}\right]\left[\text{astronomy}(t)\right]}$$

Suppose for moment that ☾, ☉ fixed in space. Then $R(t) = \text{const.}$ and $Z(t) = \text{const.}$ but $L(t) = -2\pi t/24$ hrs. due to ⊕'s rotation on its axis. This gives the lowest approx. to the tides.

Shows clearly division into 3 principal tidal species.

1. <u>semi-diurnal</u> <u>species</u> : $\cos 2(L-\phi)$
two tidal maxima and minima per day. Shape or variation on $\oplus$'s surface $\sim \sin^2\theta$

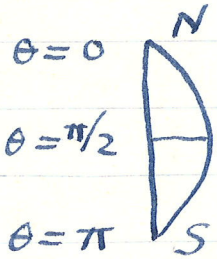

$\sin^2\theta$ zero at poles, max at equator

2. <u>diurnal</u> <u>species</u> : $\cos(L-\phi)$
one tide / day
shape on $\oplus$ surface $\sim \sin 2\theta$

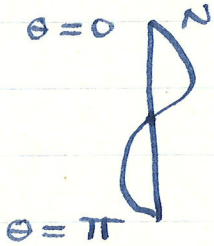

zero at poles and equator

3. <u>long-term</u> <u>species</u> : $\cos 0(L-\phi) = 1$
no variation at all if $\odot$, $☾$ fixed in sky. Actually vary slowly due to $☾$, $\odot$ motion, largest is fortnightly 2 wk. period. Shape on surface $\sim P_2(\cos\theta)$

6 months → for solar tides

$$= \frac{3}{2}\cos^2\theta - \frac{1}{2}$$

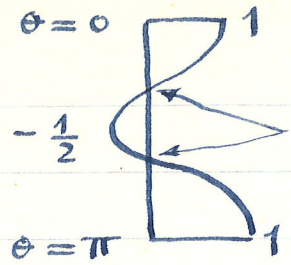

nodes at lat. 35° 16′ N and S (approx. lat. of Los Angeles)

1 at poles and $-1/2$ at equator

or, on E coast, South Carolina →

For more accurate picture of tidal variations must consider motions of ☾, ☉ in sky (geocentric view: often adopted, in spite of Copernicus, in discussing positional astronomy, a purely kinematic subject)

Principal features of ☾, ☉ motion:

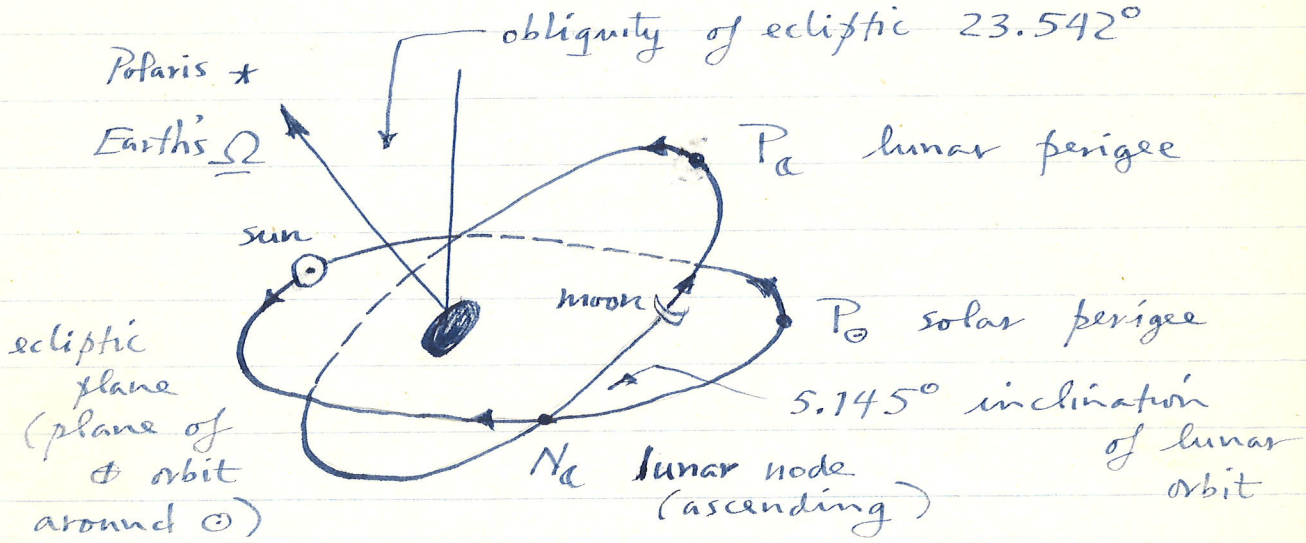

☉ goes around once per year and ☾ goes around at an inclination of ~5° to ecliptic once / month.

But due to third body effect of ☉ on ☾ and planetary perturbations (these much smaller but measurable) the orbital parameters change or evolve slowly. Three most rapid secular perturbations together with month and year comprise the:

Five fundamental celestial periods characterizing ☾ and ☉ motion:

1 month = 27.321582 msd, ☾ declination
1 (tropical) year = 365.242199 msd, ☉ declination

8.847 tropical yrs, ☾ perigee
− 18.613 tropical yrs, regression of lunar node

20,940 yrs, ☉ perigee

Next longest fundamental period is precession of equinoxes (☉'s Ω vector changes position) period ~ 25,800 yrs.

How do these celestial periods show up in the description of the equilibrium tide $h(\theta, \phi, t)$?

Consider the three terms we wrote as [astronomy (t)], viz.

$$[\cdot] = \left[(\bar{R}/R)^3 \left(\tfrac{3}{2}\cos^2 z - \tfrac{1}{2} \right) \right]$$
$$[\cdot] = \left[\tfrac{3}{4} (\bar{R}/R)^3 \sin 2z \cos(L-\phi) \right]$$
$$[\cdot] = \left[\tfrac{3}{4} (\bar{R}/R)^3 \sin^2 z \cos 2(L-\phi) \right]$$

A lengthy analytical expansion procedure allows us to write each of these factors in the form:

$$\text{astronomy}(t) = \sum_j \underbrace{C_j}_{\text{amplitude}} \cos(\sigma_j t - m\phi + \underbrace{\theta_j}_{\text{phase}})$$

$m = 0, 1, 2$ long-period, diurnal, semi-diurnal

$$\sigma_j = m\omega_\alpha + \sum_{i=1}^{5} a_i \omega_i \,, \quad a_i \text{ integers}$$

$\omega_\alpha = \Omega - \omega_1$ so $2\pi/\omega_1 = 1$ mean lunar day $= 24\,h\ 50\,m\ 28\,s$, longer than 1 solar day

$2\pi/\omega_1 = 1$ month, etc., the five fundamental periods

This a sum of harmonically varying terms. Called harmonic expansion of tidal potential, introduced by Lord Kelvin.

Use of $\omega_{☾}$, lunar day, convenient as lunar tides dominate.

Astronomy gives rise to a <u>modulation</u> of three basic tidal frequencies.
Non-linearity of celestial mechanics → sum and difference frequencies.

Each of the three tidal species split into a number of lines. A <u>line</u> <u>spectrum</u>, but line splitting actually an ∞ process, depends on how much algebra you do and how much <u>resolution</u>

One speaks of the <u>resolution</u> of any particular development. Results most easily presented in <u>line</u> <u>spectrum</u> form. At <u>1 cpd</u> <u>resolution</u>, lowest approx., <u>corresponds to a, ⊙ motionless in space</u>.

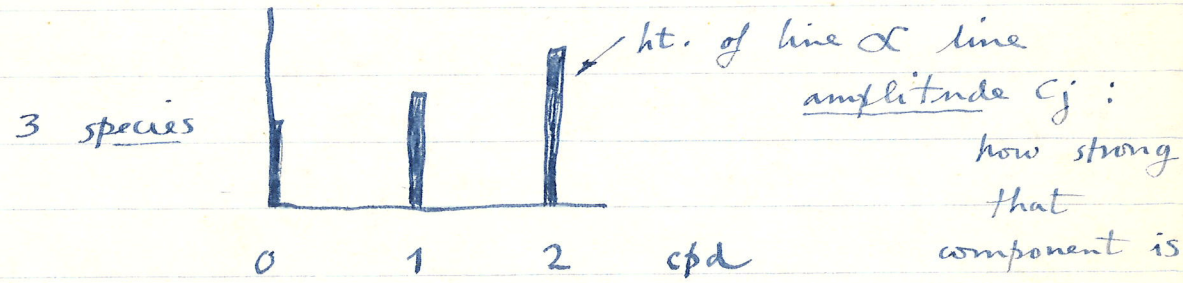

At <u>1 cpm resolution</u> see <u>fortnightly</u> splitting — each line now called a <u>group</u>

minimum spacing now $2\pi/2\omega_1 = 13.661$ days ~ 2 wks (fortnight)

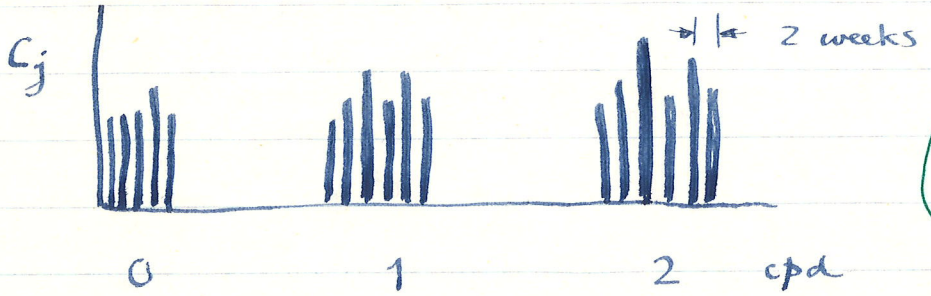

This equivalent to assuming ☾, ☉ orbits are Keplerian (unchanging elliptical elements).

At 1 cpy resolution one sees annual splitting of each group — each line now called tidal constituent. Minimum spacing now 1/2 years.

Harmonic expansion first suggested by Kelvin, carried out by G. Darwin ~ 1860's to largest 39 terms, smallest $c_j \sim 10^{-3}$ largest. Gave names to various constituents, still in use, e.g.

M_2 ☾ semi-diurnal
M_f ☾ fortnightly
S_2 ☉ semi-diurnal

A.T. Doodson of Admiralty Office 1921 Proc. Roy. Soc. carried out expansion further to largest 400 c_j, smallest ~ 10^{-4}. largest. He worked to ☉ perigee resolution i.e. found exact speed

of each term, but truncated sum at largest 400.
This a monumental task: 20 years of work on a hand calculator, Doodson's lifes work.

His notation (slightly modified) is convenient. Identify a line by its Doodson number:

$$\boxed{\text{Doodson number} = (m, a_1, a_2, a_3, a_4, a_5)}$$

Table of a few of the largest lines:

Doodson	Darwin	period	☾ or ☉	C_j
Long-period:				
020000	M_f	13.661 d	☾	.1564
010-100	M_m	27.555 d	☾	.0825
Diurnal:				
110000	K_1	1 sidereal day	both	.5305
1-10000	O_1	25.819 hrs.	☾	.3769
Semi-diurnal:				largest ☾
200000	M_2	12.421 hrs.	☾	.9081
22-2000	S_2	12 hrs.	☉	.4229
				largest ☉

K_1 at 1 sidereal day = 23h 56m 04s only tidal line due to both ☾ and ☉. (also K_2 twice/sid. day)

Show Munk + Cartwright figures of equilibrium spectrum at 1 cpm and 1 cpy resolution. Also plotted are observations of ocean tide at Honolulu, mid-Pacific ocean station. Note noise continuum of meteorological origin.

Also show fortnightly tidal gravity variation measured at South Pole by Louis Slichter.

Final Munk + Cartwright figure shows nodal splitting of Sa and Ssa semi-annual and annual lines.

N, the nodal tide, period of 18.6 years.

Note the hint of a pole tide at 14 months, response of the oceans to the Chandler wobble not forced by ☾ or ☉.

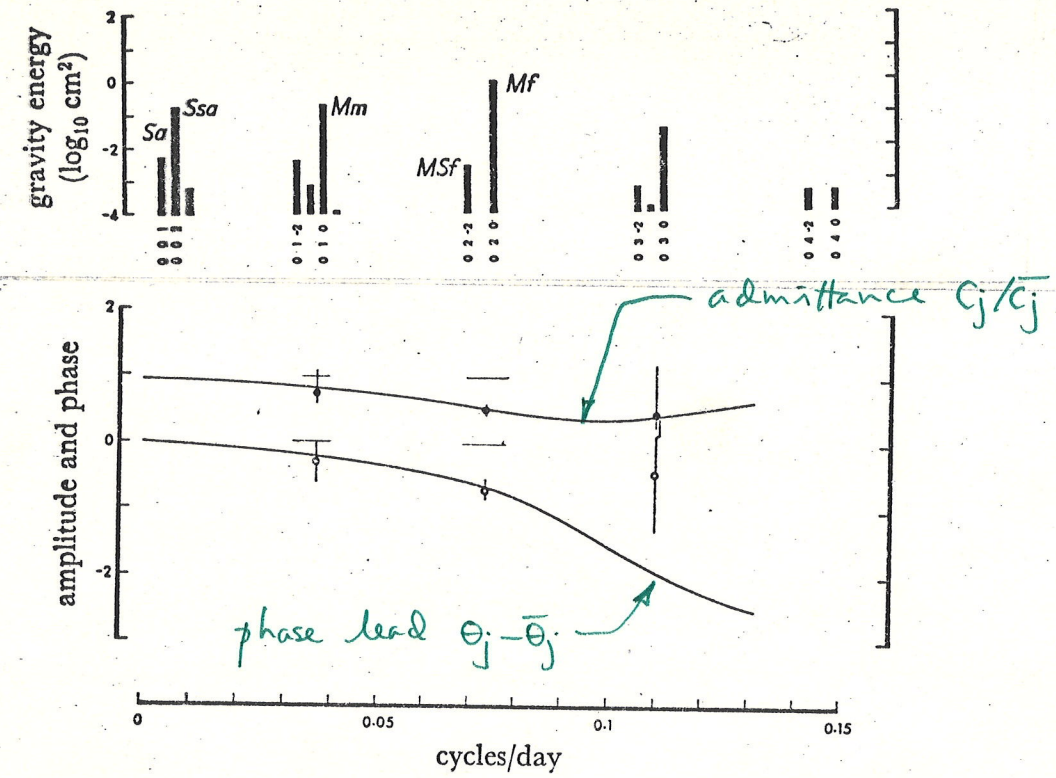

Figure 2. Honolulu tide spectra at 1 c/y resolution for the low-frequency spherical harmonic P_2^0. Some 'Darwin' symbols and 'Doodson' constituent numbers are included in the upper panel. Legend is otherwise as in figure 1.

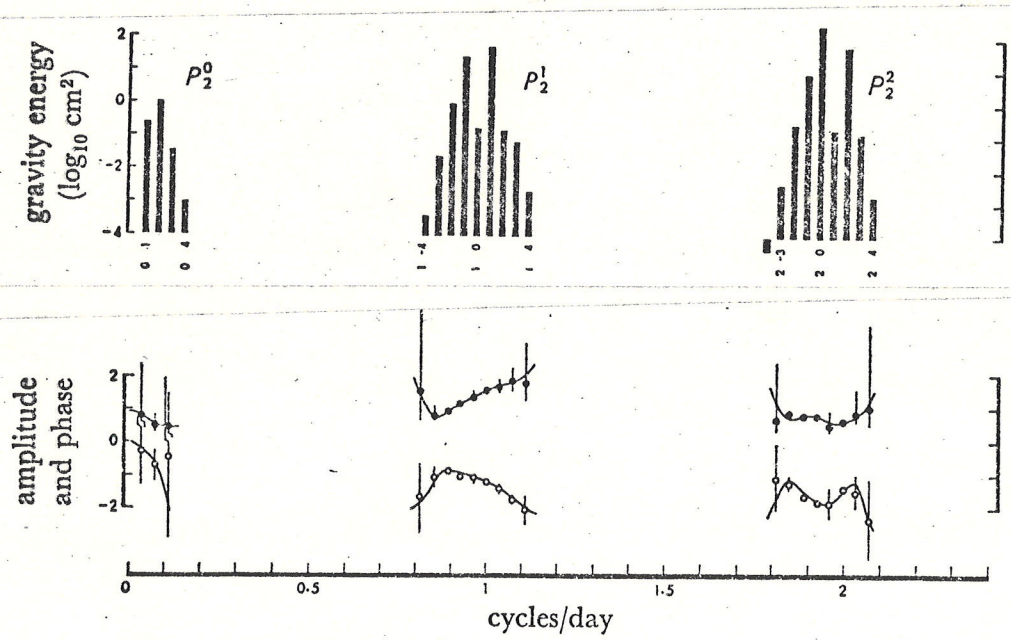

Figure 1. Honolulu tide spectra at 1 c/m resolution for spherical harmonics of degree 2. P_2^0, P_2^1, P_2^2, refer to tidal species 0, 1, 2 respectively. The upper panel shows the energy of the gravitational equilibrium tide at Honolulu relative to 10^{-4} cm^2; some 'Doodson group numbers' are written below the columns. In the next two panels, the observed sea spectrum is designated by the total height of the columns. In the upper of the two, the height of the *filled* portion designates the energy *coherent* with the equilibrium tide; in the lower, the height of the *unfilled* portion designates the *noncoherent* energy. The left scale refers to energy per column, the right scale to energy per c/d. In panel 4, the filled circles refer to the real part, the open circles to the imaginary part of the admittance. In panel 5, they refer to |admittance| and phase lead in radians, respectively. The vertical lines show the 95 % confidence limits of the circles. The curves represent the admittance functions derived from the convolution process.

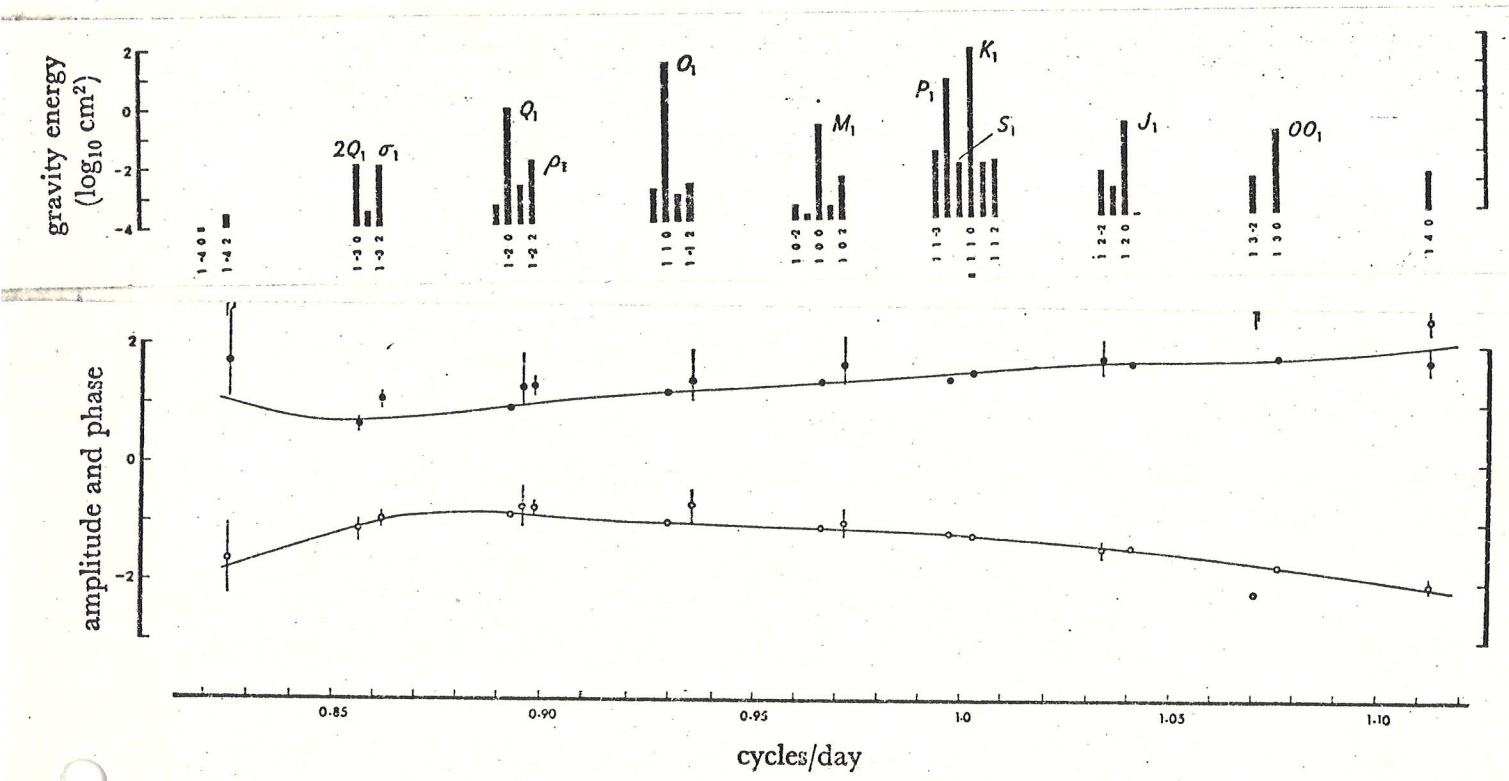

FIGURE 3. Honolulu tide spectra at 1 c/y resolution for the diurnal spherical harmonic P_2^1.

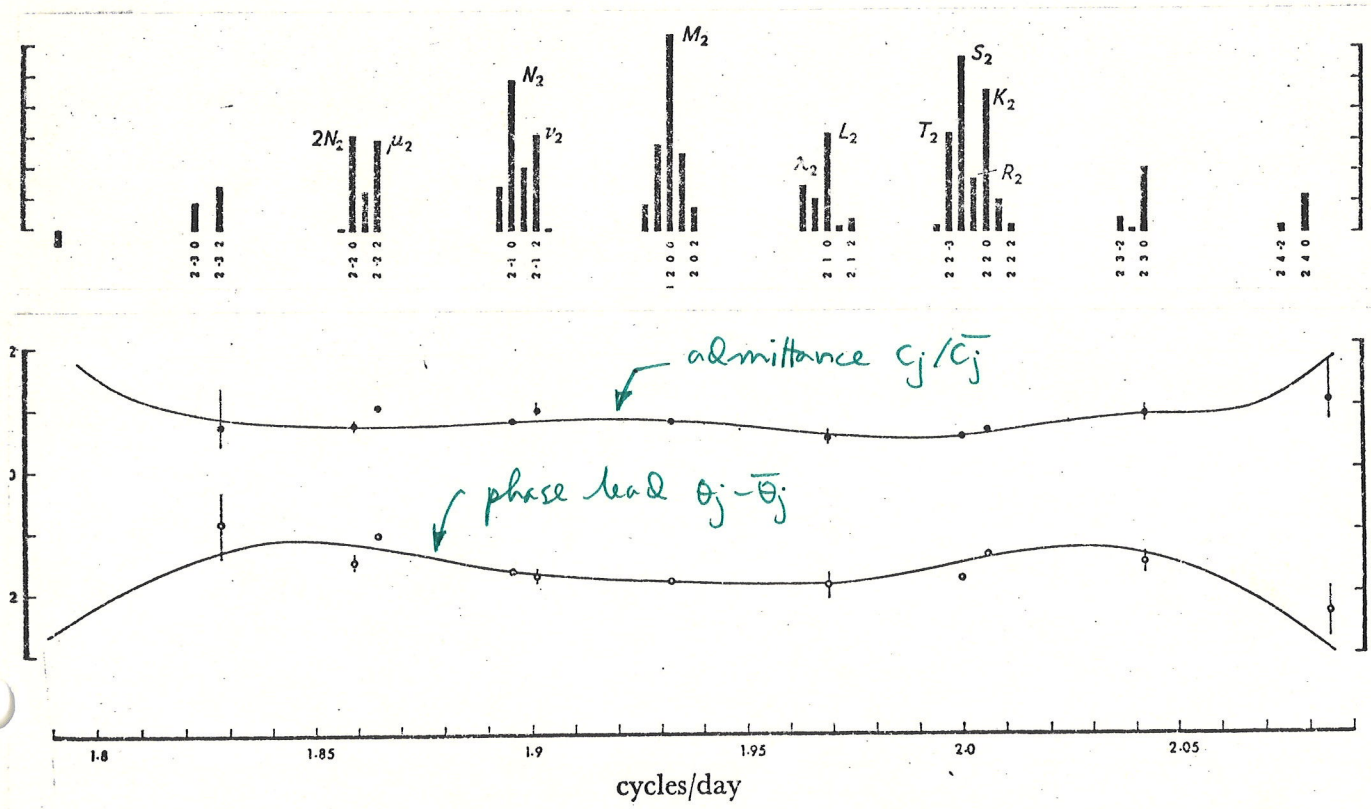

FIGURE 4. Honolulu tide spectra at 1 c/y resolution for the semidiurnal spherical harmonic P_2^2.

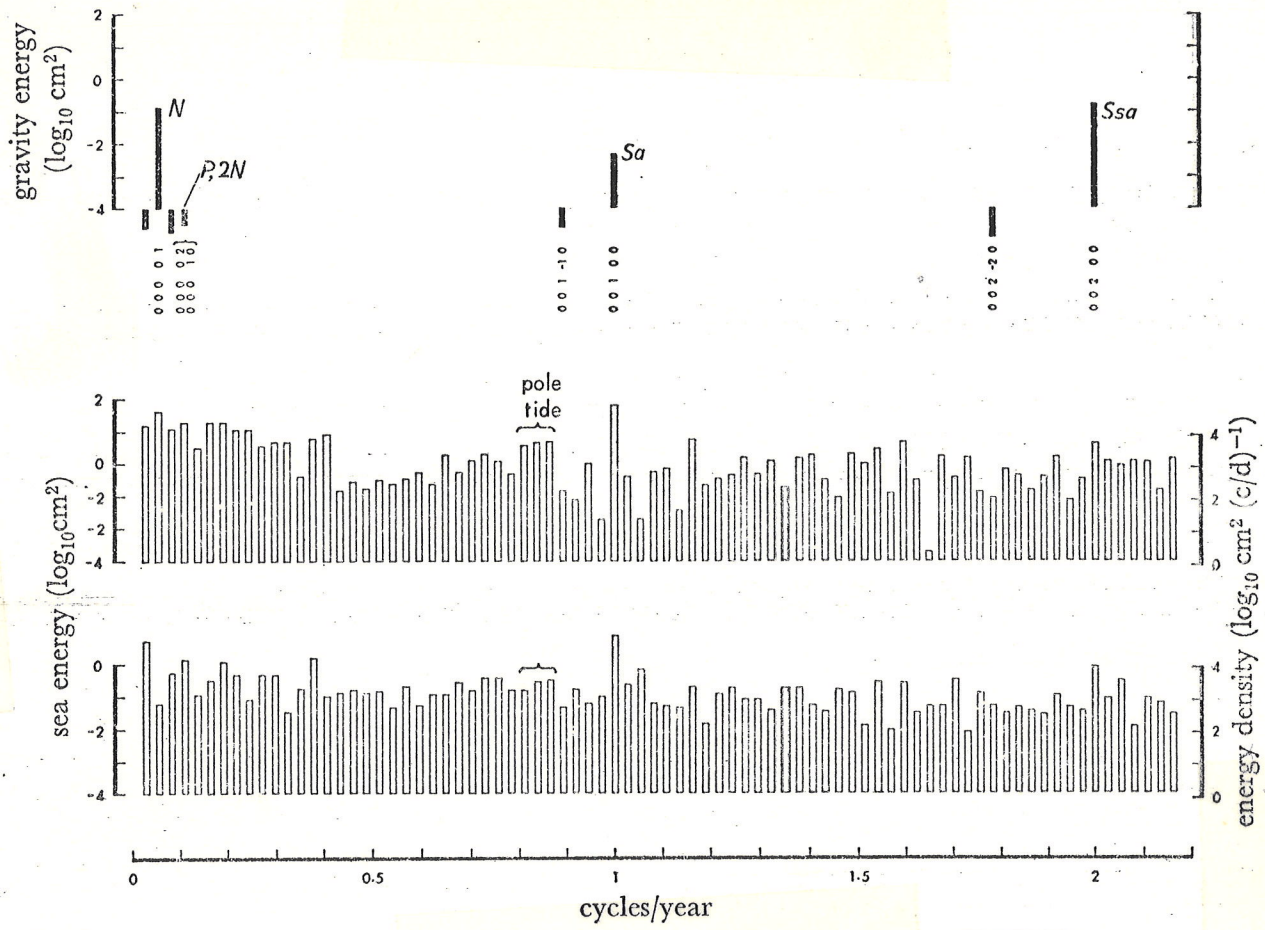

TABLE 2.4.4. Tidal constituents with $C > 0.05$ (from [Bartels, 1957])

Coefficient C	Speed (deg hr^{-1}) σ	Period $360°/\sigma$	Symbol (and description)
	Long-period tides		
0.2341	0		S_0 (constant solar)
0.5046	0		M_0 (constant lunar)
0.0655	$\omega_4 = 0.00221$	18.613 years	— (nodal to M_0)
0.0729	$2\omega_2 = 0.08214$	182.621 days	*Ssa* (declinational to S_0)
0.0825	$\omega_1 - \omega_3 = 0.54437$	27.555	*Mm* (elliptical to M_0)
0.1564	$2\omega_1 = 1.09803$	13.661	*Mf* (declinational to M_0)
0.0648	$2\omega_1 + \omega_4 = 1.10024$	13.633	— (nodal to *Mf*)
	Diurnal tides		
0.0722	$(\omega_☾ - \omega_1) - (\omega_1 - \omega_3) = 13.39866$	26.868 hours	Q_1 (elliptical to O_1)
0.0710	$(\omega_☾ - \omega_1) - \omega_4 = 13.94083$	25.823	— (nodal to O_1)
0.3769	$(\omega_☾ - \omega_1) = 13.94304$	25.819	O_1 (principal lunar)
0.1755	$(\omega_\odot - \omega_2) = 14.95893$	24.066	P_1 (principal solar)
0.1682	$(\omega_\odot - \omega_2) + 2\omega_2 (= \Omega) = 15.04107$	23.934	K_1^S (declinational to P_1)
0.3623	$(\omega_☾ - \omega_1) + 2\omega_1 (= \Omega) = 15.04107$	23.934	K_1^M (declinational to O_1)
0.0718	$(\omega_☾ + \omega_1) + \omega_4 = 15.04328$	23.931	— (nodal to K_1^M)
	Semidiurnal tides		
0.1739	$2\omega_☾ - (\omega_1 - \omega_3) = 28.43973$	12.658 hours	N_2 (elliptical to M_2)
0.9081	$2\omega_☾ = 28.98410$	12.421	M_2 (principal lunar)
0.4229	$2\omega_\odot = 30$	12	S_2 (principal solar)
0.0365	$2\omega_\odot + 2\omega_2 (= 2\Omega) = 30.08214$	11.967	K_2^S (declinational to S_2)
0.0786	$2\omega_☾ + 2\omega_1 (= 2\Omega) = 30.08214$	11.967	K_2^M (declinational to M_2)
	Combination tides		
0.5305	$\Omega = 15.04107$	23.934 hours	K_1 (lunisolar declinational)
0.1151	$2\Omega = 30.08214$	11.967	K_2 (lunisolar declinational)

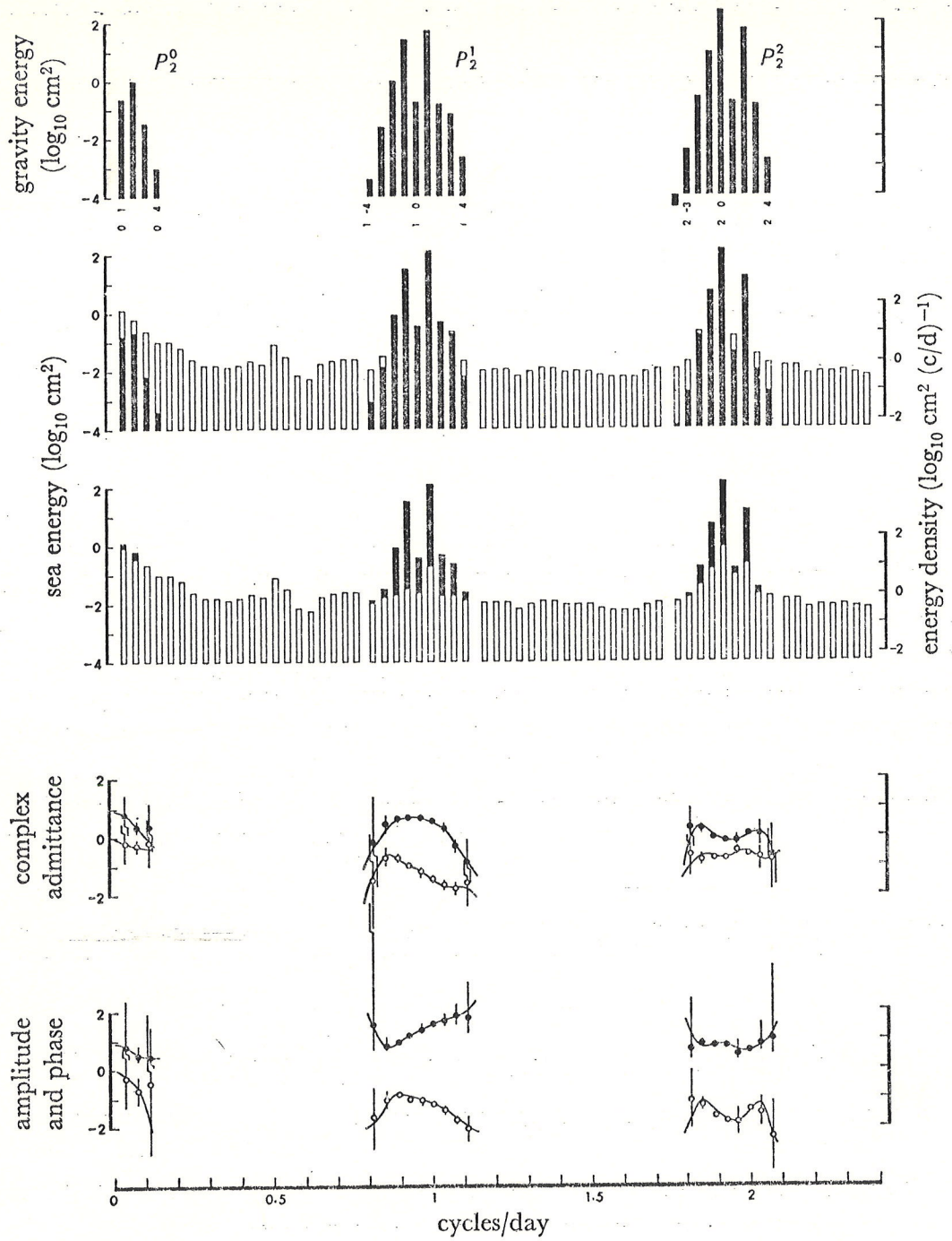

FIGURE 1. Honolulu tide spectra at 1 c/m resolution for spherical harmonics of degree 2. P_2^0, P_2^1, P_2^2, refer to tidal species 0, 1, 2 respectively. The upper panel shows the energy of the gravitational equilibrium tide at Honolulu relative to 10^{-4} cm^2; some 'Doodson group numbers' are written below the columns. In the next two panels, the observed sea spectrum is designated by the total height of the columns. In the upper of the two, the height of the *filled* portion designates the energy *coherent* with the equilibrium tide; in the lower, the height of the *unfilled* portion designates the *noncoherent* energy. The left scale refers to energy per column, the right scale to energy per c/d. In panel 4, the filled circles refer to the real part, the open circles to the imaginary part of the admittance. In panel 5, they refer to |admittance| and phase lead in radians, respectively. The vertical lines show the 95 % confidence limits of the circles. The curves represent the admittance functions derived from the convolution process.

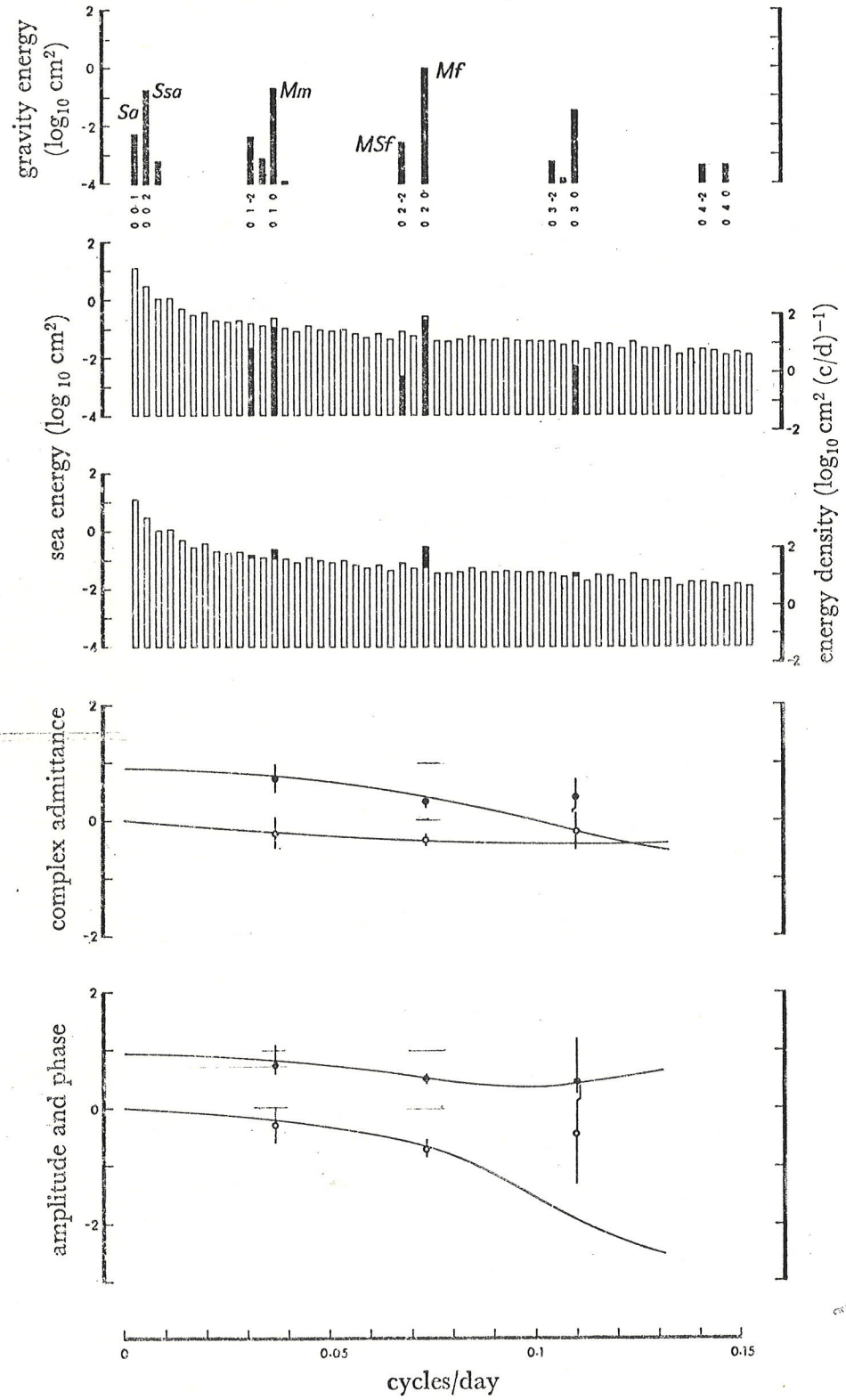

FIGURE 2. Honolulu tide spectra at 1 c/y resolution for the low-frequency spherical harmonic P_2^0. Some 'Darwin' symbols and 'Doodson' constituent numbers are included in the upper panel. Legend is otherwise as in figure 1.

(c) *The spectrum at c/y resolution*

Figures 2 to 4 show the same spectra and admittances at greater resolution. Here we see the tidal 'constituents' named by Darwin and other constituents of lesser importance, usually unnamed or allocated to nonlinear 'over-tides'. In figure 2, the constituent labelled *MSf* is the linear lunar input at (0 2 −2), not the S_2-M_2 nonlinear interaction at the same frequency. The coherent energies at 1 and 2 c/y (*Sa* and *Ssa*) were not plotted because they

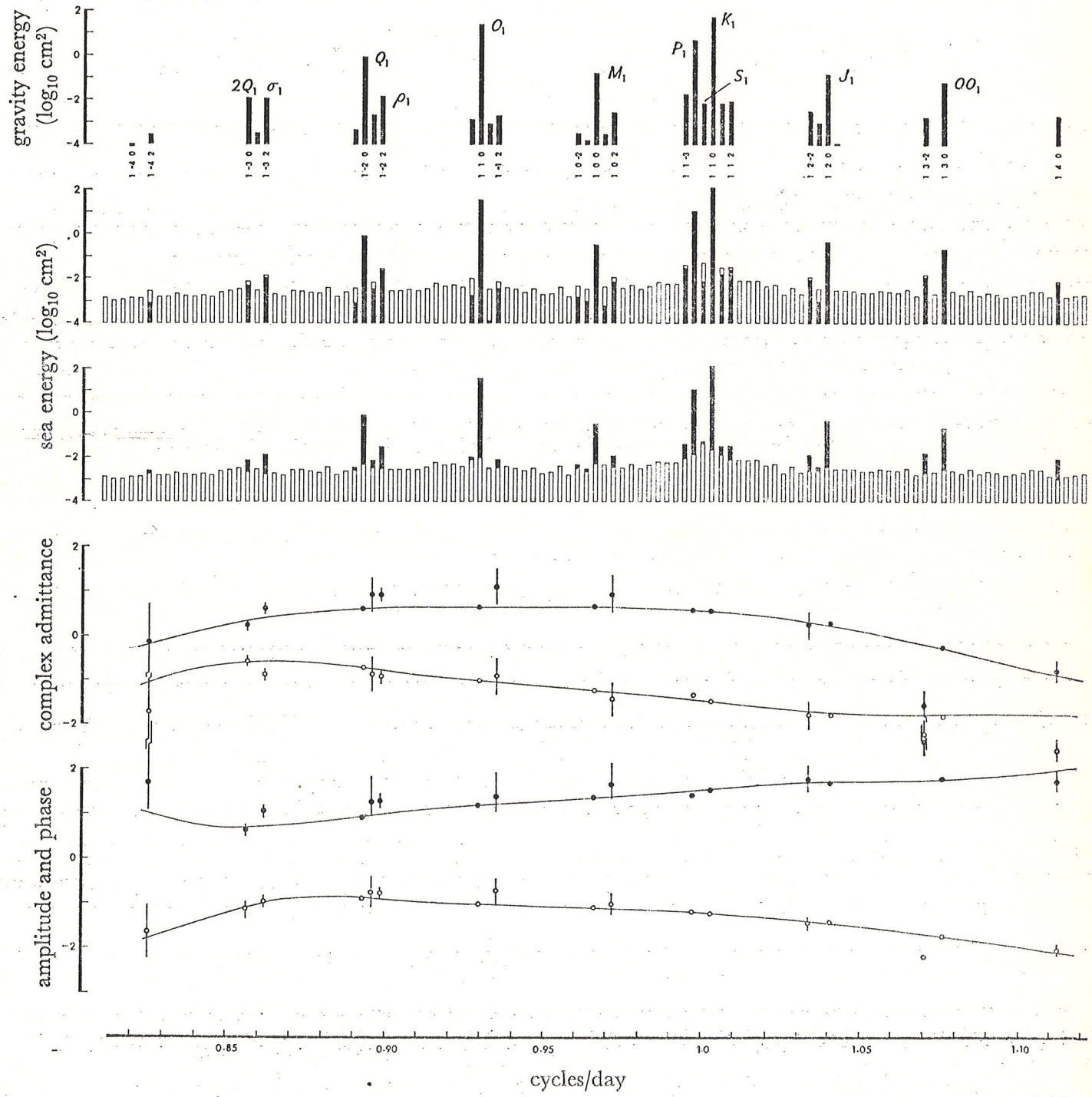

FIGURE 3. Honolulu tide spectra at 1 c/y resolution for the diurnal spherical harmonic P_2^1.

include radiational energy and give anomolous admittances. Separation of gravitational and radiational energy is possible by the method of multiple components. A better procedure is the lumped analysis on which the plotted curves are based. These curves approach a gravitational admittance of $Z = 0{\cdot}92$ at zero frequency. The reliability of this limit is about the same as that of the estimate at 1 c/m, namely $\pm 0{\cdot}24$ at the 95 %

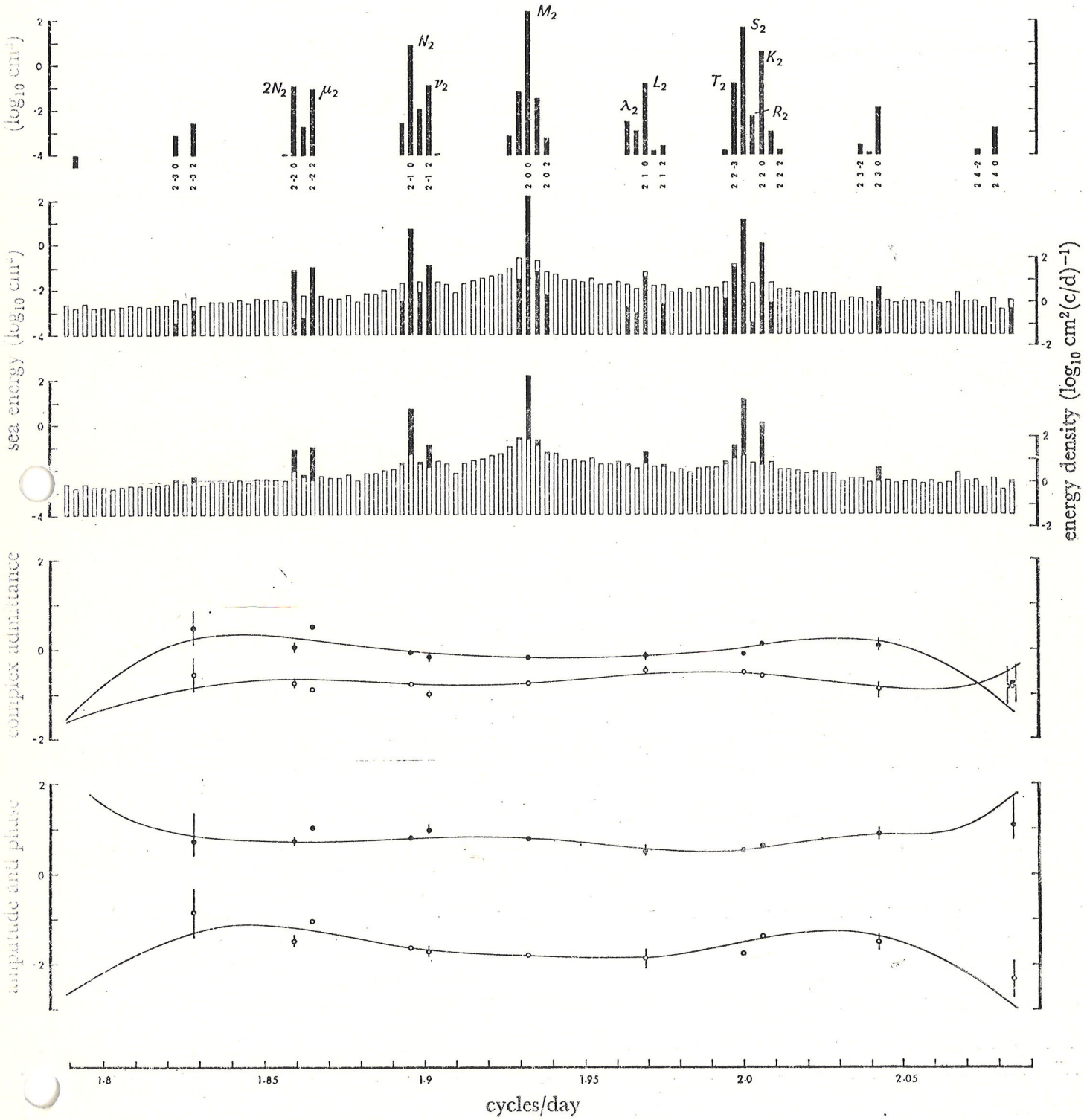

FIGURE 4. Honolulu tide spectra at 1 c/y resolution for the semidiurnal spherical harmonic P_2^2.

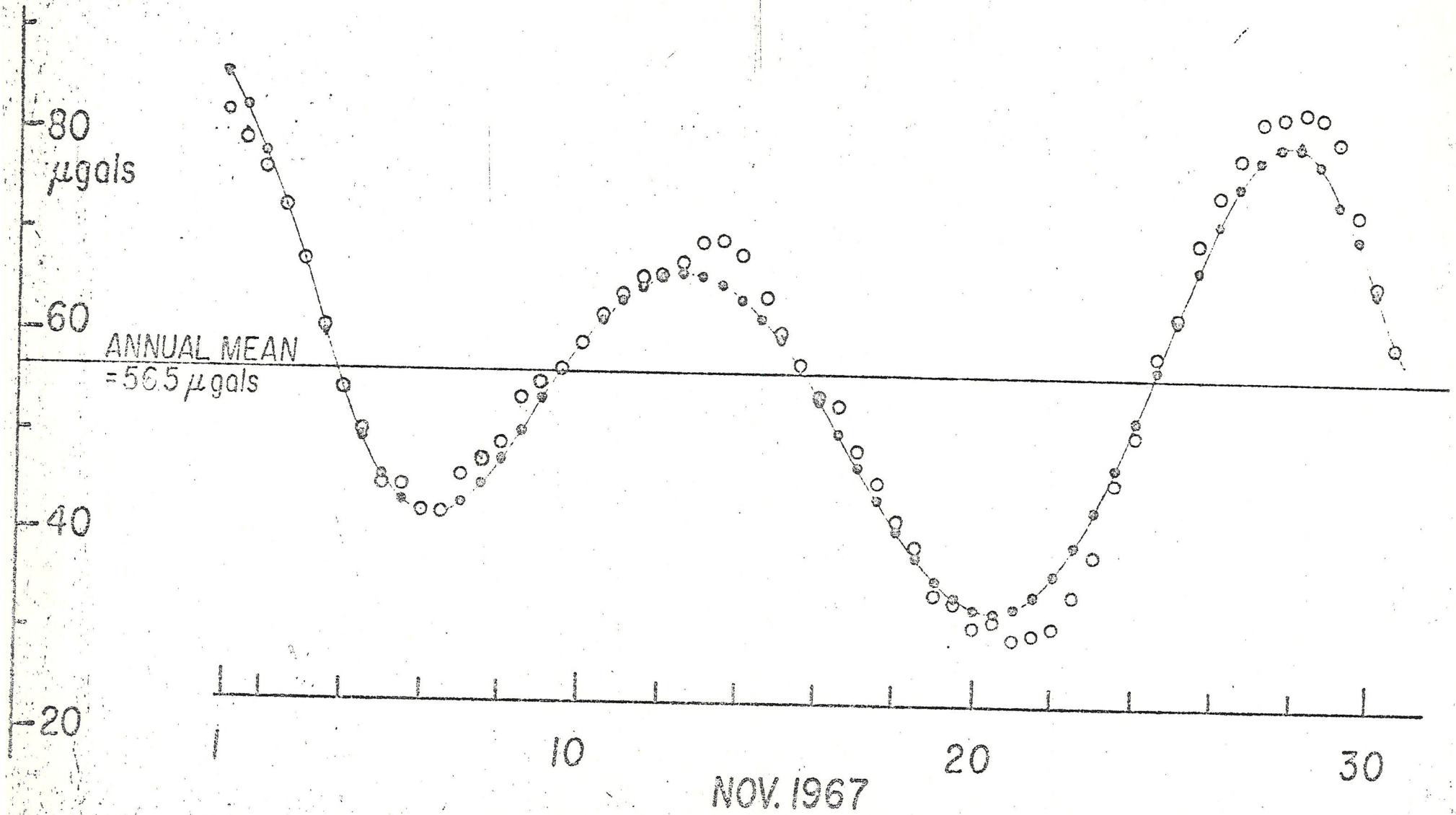

GRAVITY TIDE, SOUTH POLE

Tidal prediction

We now have obtained a complete description of cause of tides; the equilibrium tide is a description of tidal forcing or input. We now turn to response of ⊕ and oceans to this forcing.

First, a subject of commercial importance, although less so today than in days of sailing ships.

Long before the scientific theorizing, ∃ rule of thumb methods of tidal prediction. These considered gainful family possessions, father → son, methods undivulged, presumably a form of regression, tides described by a few relevant variables (time, ht. of high and low water, etc.), relate to a few astron. variables (phase, declination of ☾, etc.)

Harmonic method developed by Kelvin and Darwin ~ 1860–1870, has a physical basis.

Assumes only that a port's response to tidal input is linear. Let us now denote equil. tide by $\bar{h}(\theta, \phi, t)$

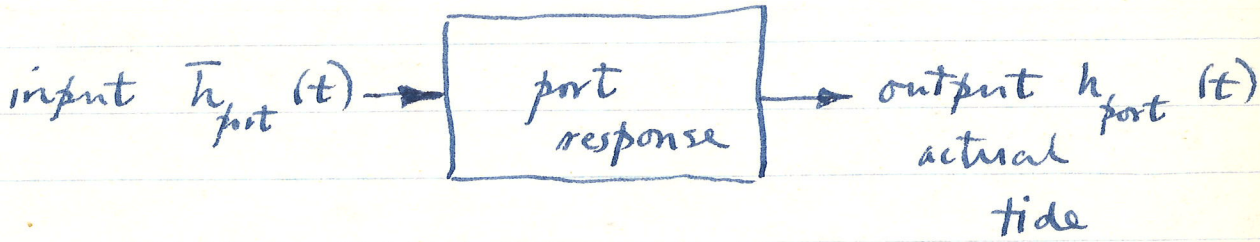

This the <u>reason</u> for harmonic development. Input at any port

tidal frequencies: $\sigma_j = m\omega_\oplus + \sum_{i=1}^{5} a_i \omega_i$

$$\bar{h}(t) = \sum_j \bar{C}_j \cos(\sigma_j t + \bar{\theta}_j)$$

amplitude

phase (called $-m\phi_{port} + \theta_j$ before).

A <u>linear</u> black box cannot change freq. of input. Resonances can alter <u>amplitude</u> of any harmonic input and resonance + friction can alter <u>phase</u>. One assumes also that $h(t)$ at any port depends only on $\bar{h}(t)$ <u>at the port</u>. Then $h(t)$ must be of form:

amplitude

phase

$$h(t) = \sum_j C_j \cos(\sigma_j t + \theta_j) \quad \star$$

tidal frequencies

At any port can determine amplitudes and phases of each line (M_2, etc.) by analysis of historical tidal records. Then to predict just extrapolate * into future.

Darwin found 39 most important frequencies. By early 1900's method well-established, today in common use. Doodson noted that after removal of 39 terms many ports still showed strong harmonic residuals. Decided it was worthwhile to find next most important frequencies (went to 400, 20 yrs. of work)

Kelvin invented mechanical analogue machines (predecessor of computer) for harmonic analysis of past tidal records (dial a speed or Doodson number, trace curve, find c_j, θ_j), also invented similar machine for drawing tidal predictions. Samples of both on display in Smithsonian in D.C.

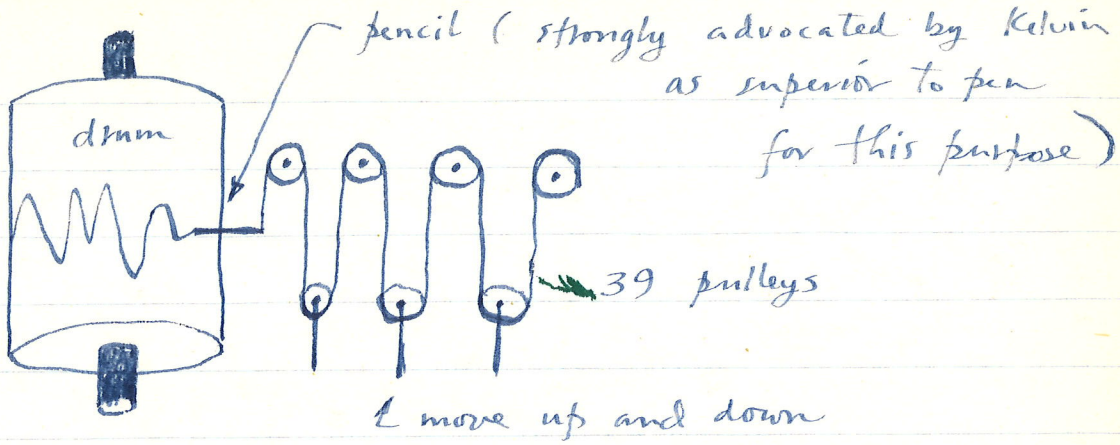

amplitude c_j, phase θ_j, i.e. $c_j \cos(\sigma_j t + \theta_j)$

Reset c_j, θ_j of lower pulleys for any port "... can run off the tides for 1 yr in about 4 hrs."

Harmonic method still for most part in use today for practical tidal prediction. Uses digital electronic computers for analysis.

To what extent do observed tides resemble equilibrium? Question is: how close are observed c_j, θ_j to $\bar{c}_j$, $\bar{\theta}_j$?

<u>Admittance</u> defined by $c_j / \bar{c}_j$, resonance factor.
Coastal admittances can be up to 10 in places.

Even in mid-ocean tides are truly a resonant phenomenon.

<u>Example</u> : Honolulu semi-diurnal admittance varies from 1/2 to 1 1/2, phase lag $\theta_j - \overline{\theta}_j$ ± 2 radians or more than 90°.

At some ports non-linear interactions dominate and linear prediction does not work well.

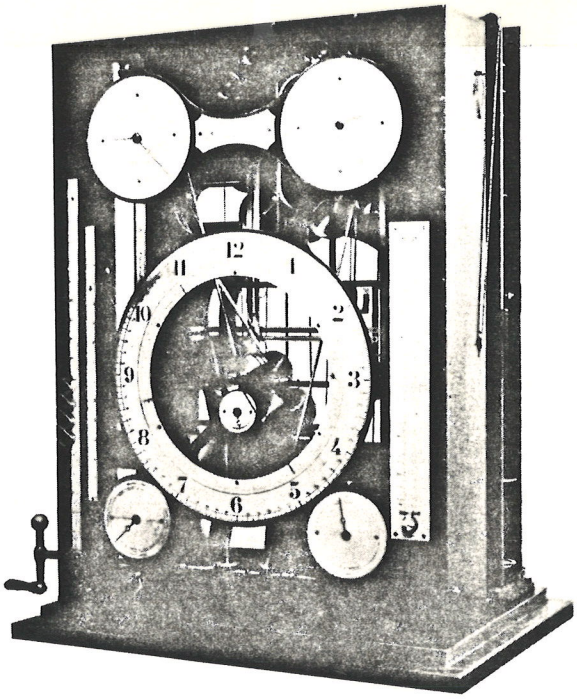

Figure 7. Tide predicting machine used from 1885 through 1914.

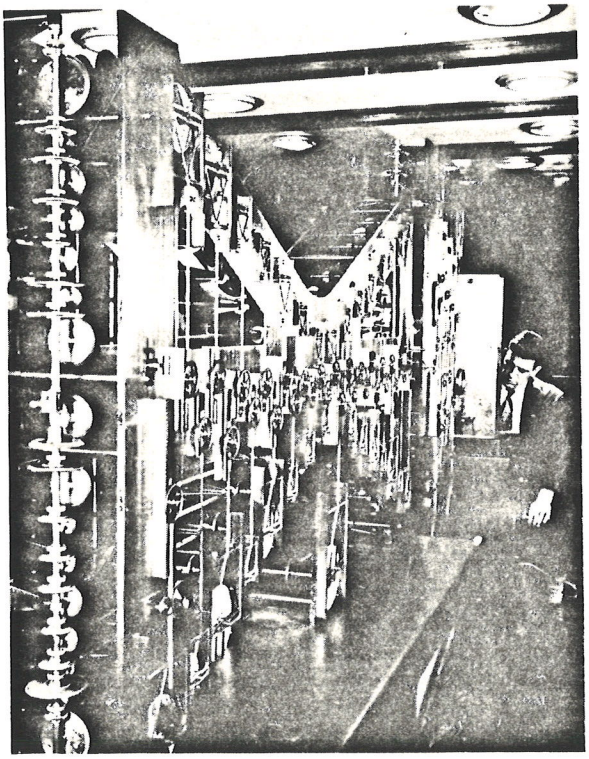

Figure 8. Tide predicting machine used from 1912 through 1965.

Response of the solid Earth : Love numbers

We shall now assume :

1. ⊕ has no oceans
2. ⊕ is spherically symmetric

Such an ⊕ may be described completely for our purposes by three parameters (for any purpose where response is elastic – time scales of a few yrs. or less).

Three parameters :

1. density $\rho(r)$

2. incompressibility or bulk modulus $\kappa(r)$: a measure of ability to withstand compression.

Conceptual measurement (defn.) :
Sphere of material, volume V.

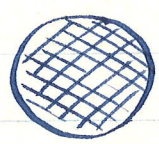

pressure P

compression changes volume by ΔV

The bulk modulus is defined by

$$P = \kappa\,(\Delta V/V)$$

fractional change in volume

pressure applied to outside

The more a material can withstand compression the greater is the <u>incompressibility</u> κ

3. <u>rigidity</u> or <u>shear modulus</u> μ (r): a measure of ability to withstand <u>shear</u>. Conceptual measurement

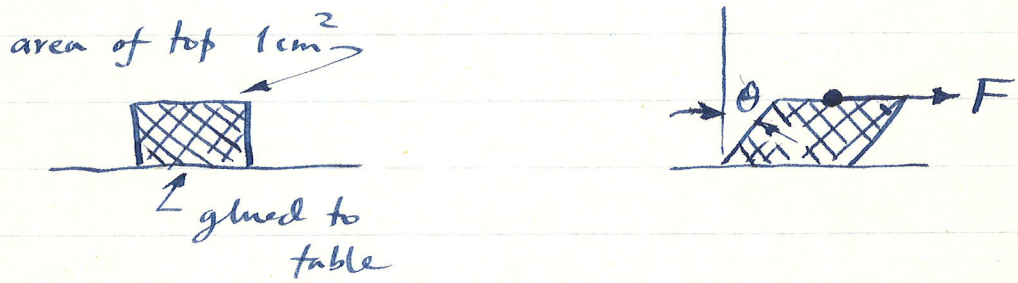

Apply a shearing force F to top of block. Shears by an angle θ. Rigidity is:

$$F/A = 2\mu\theta$$

amount of shear

shear force per unit area

For a <u>fluid</u> no rigidity at all
$\mu = 0$, e.g. air, H_2O,
molten Fe of ⊕'s core.

Units of κ and μ force/area, dyne/cm^2.
Typical values

	κ	μ
H_2O	$0.2 \cdot 10^{11}$ dyne/cm^2	0
granite	$5.5 \cdot 10^{11}$	$2 \cdot 10^{11}$
steel	$17 \cdot 10^{11}$	$8 \cdot 10^{11}$

We shall assume solid ⊕ response is <u>equilibrium</u> since period of $_0S_2$ $\ll$ 12 hrs.

Plots of $\rho(r)$, $\kappa(r)$, $\mu(r)$ for a modern ⊕ model (PEM) Figures 6.17 and 6.18 of Stacey, units 10^{11} Pa or 10^{12} dyne cm^{-2}.
Features: all increase by about one order of magnitude in mantle, $\mu = 0$ in fluid core, note solid inner core.

Tidal potential deforms ⊕. The <u>surface</u> deformation can be conveniently

precision of observations, the lower mantle and the outer core were each homogeneous and obeyed the Adams-Williamson equation (see also Davies and Dziewonski, 1975). The density profile of one model is shown in Figure 6.17.

Inferences concerning the compositions of the interior zones of the Earth require extrapolation of the model densities to zero pressure.

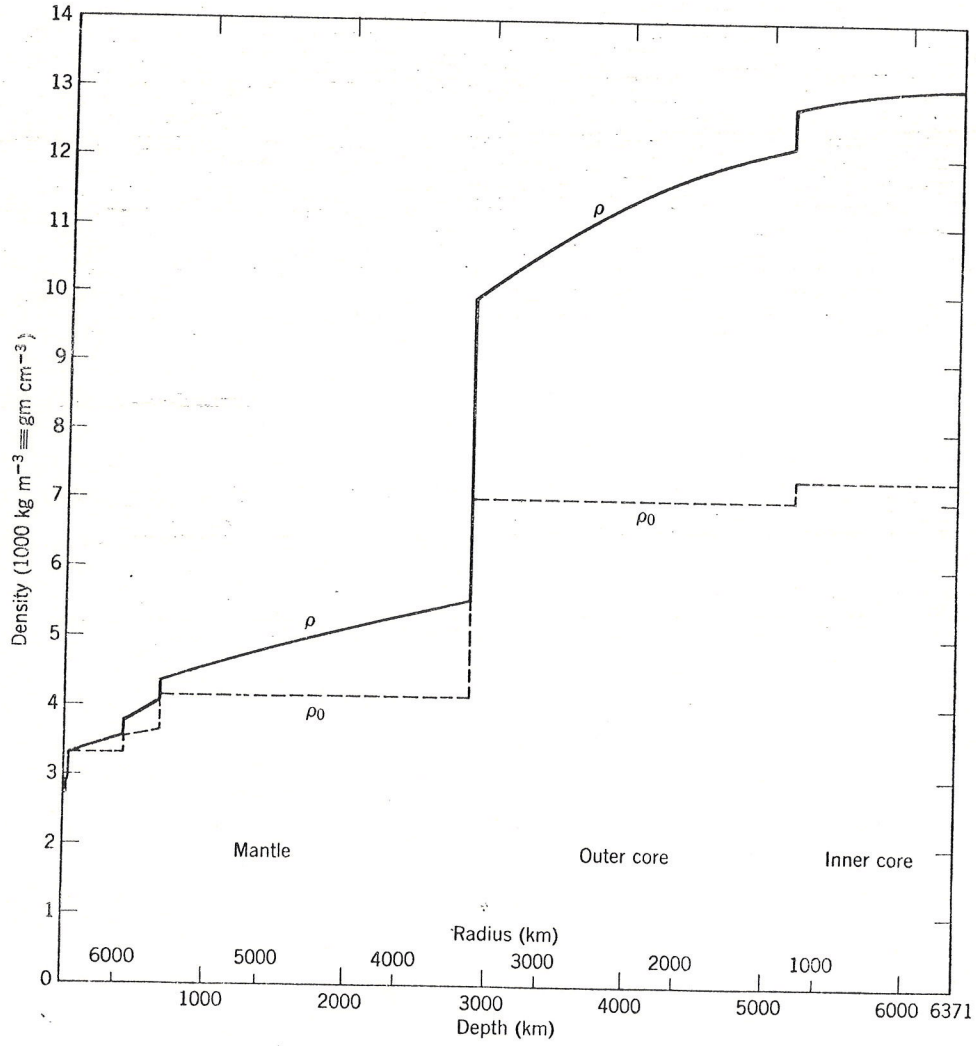

Figure 6.17. Density profile of Earth model by Dziewonski et al. (1975) (solid line) with corresponding extrapolated zero pressure (and room temperature) density (broken line).

Conventional elasticity theory, which assumes infinitesimal strain, is completely inadequate for this purpose because the elastic constants change dramatically under pressures comparable in magnitude to the elastic moduli. There are first-order changes in density, which can be described only by a finite strain theory. Figure 6.18 is a plot of the elastic moduli within the Earth as functions of pressure. This shows that the variations with pressure are sufficiently regular for simple linear relationships to represent reasonably well the behavior over moderate pressure ranges:

$$K = K_0 + K_0' P \tag{6.39}$$

$$\mu = \mu_0 + \mu_0' P \tag{6.40}$$

where subscripts 0 represent zero pressure values. In particular, for the upper part of the lower mantle (from 670 km to about 1500 km according

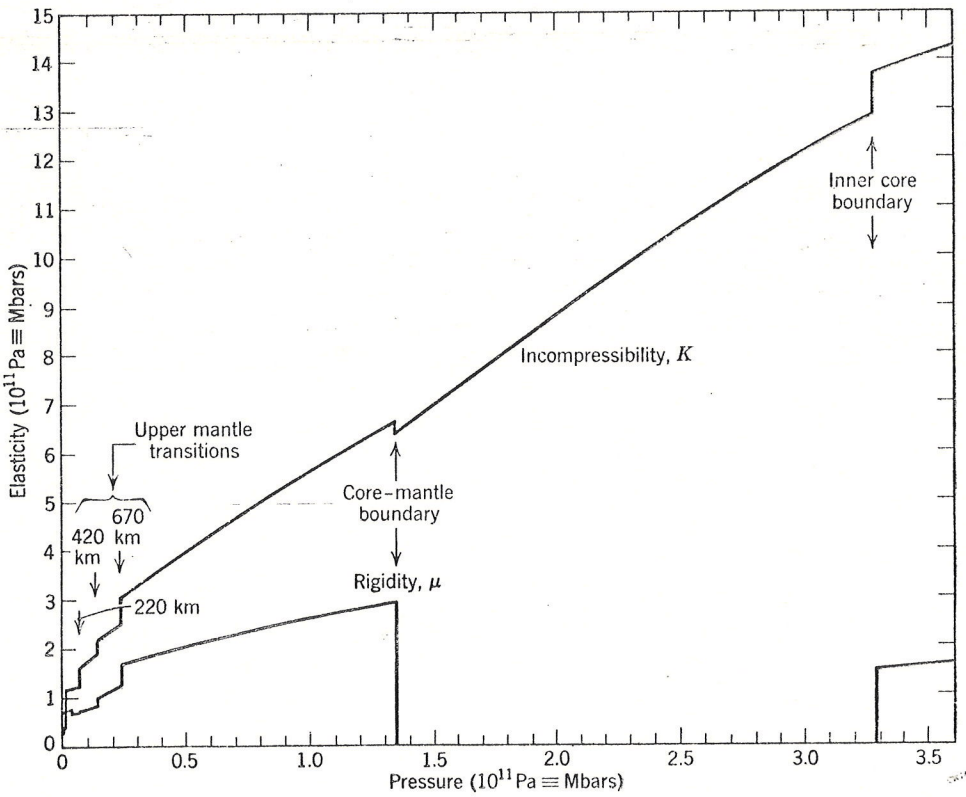

Figure 6.18. Variations of elastic constants with pressure in the interior of the Earth (model data by Dziewonski et al. 1975—Appendix G).

characterized in terms of 3 parameters, <u>Love numbers</u>, which summarize elastic response of ⊕ to tidal ($l = 2$) forces.

The <u>surface</u> $r = a$ will be displaced

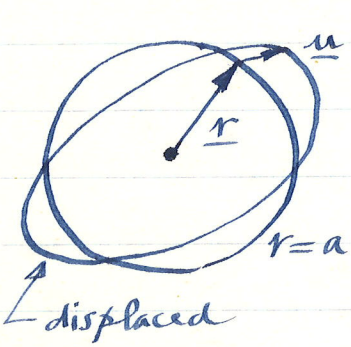

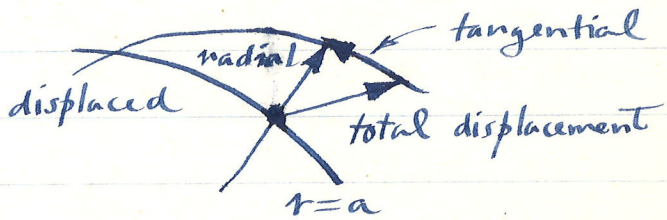

This the ⊕ surface (<u>the ground</u>) being displaced, not equipot. surface.

Let $\hat{r} \cdot \underline{u}(\underline{r}) = u_r(\underline{r})$ = radial displacement

Since ⊕ a <u>linear</u> system

$$\boxed{u_r(\underline{r}) = -h \underbrace{\left[\frac{V(\underline{r})}{g}\right]}_{1 \text{ equil. tide}}}$$

Love number

Twice as big a force → twice as much displ.

Note ⊕ "bulges" where the tidal bulge "bulges".

$h > 0$ for a realizable model.
Actual no. depends on
model $\rho(r)$, $\kappa(r)$, $\mu(r)$
in a complicated way.

For real ⊕ : $h \sim 0.\cancel{3}$ 0.6 (.$\cancel{300}$ 0.609 1066A, B)
For rigid ⊕ : $h = 0$, no deformation at all.

For incompr. <u>fluid</u> ⊕ : $\kappa = \infty$, $\mu = \text{const.}$
$\rho = \text{const.}$

fluid
μ, ρ

$h = 5/2$

$\kappa = \infty$ not a bad approx for ⊕ <u>for this application</u>.
even though actually only about two times μ.

<u>Tangential displacement</u> has two components. Let θ, ϕ be polar coords on $r = a$

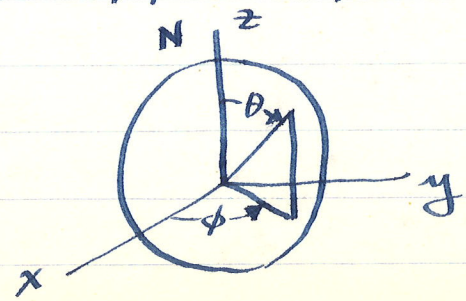

θ = colatitude
ϕ = longitude

Then 2 comps. of tang. displ. are:

$$\hat{\theta}: \quad -\ell\left[\frac{1}{g}\frac{\partial V(\theta,\phi)}{\partial\theta}\right]$$

$$\hat{\phi}: \quad -\ell\left[\frac{1}{g}\frac{1}{\sin\theta}\frac{\partial V(\theta,\phi)}{\partial\phi}\right]$$

Love number

Rigid $\oplus$: $\mu = \infty$, $\ell = 0$
Real $\oplus$: $\ell \sim 0.08$ (0.085 10GCA, B)

We shall not make use of this Love number further, not introduced by Love but by Shida.

Another quantity of interest is the resulting change in the net grav. pot. at $r = a$ Total pot. is

$$\phi(\underline{r}) = \phi_0(\underline{r}) + (1+k)\,V(\underline{r})$$

due to undeformed $\oplus$ (equal to $-\frac{GM_\oplus}{a}$ on $r=a$)

Love number

the applied tidal potential

k measures additional pot. due to <u>redistribution</u> of <u>mass</u> of ⊕

Rigid ⊕ : $k = 0$, no redistribution
Real ⊕ : $k \sim$ ~~0.6~~ 0.3 (~~0.609~~ 0.300 1066 A, B)
Incompr. fluid ⊕ : $k = 3/2$

k and h introduced by A.E.H. Love ~ 1900. Together k, l, h characterize <u>equil.</u> response of spherical ⊕ to an applied $l = 2$ potential. They are <u>dimensionless</u> numbers, a neat way of <u>summarizing</u> elastic response of ⊕.

Their importance: <u>any</u> measurement of tidal response on ⊕ surface can be expressed in terms of h, l, k.

Tidal measurements: first example, suppose ∃ a grav. <u>potentiometer</u>, could measure grav. <u>potential</u> (actually no such instrument exists but this simplest case to consider).

The instrument is on ⊕ surface which moves.

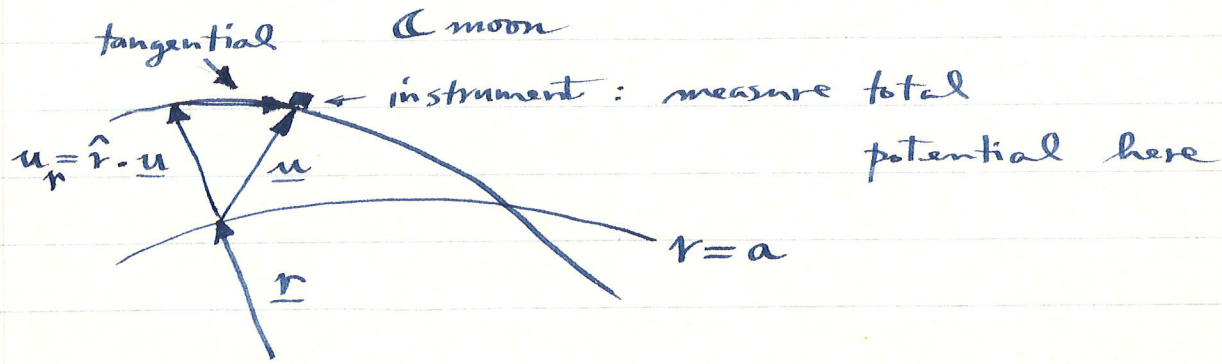

Total potential at $\underline{r} + \underline{u}$ is (Taylor series)

$$\phi(\underline{r} + \underline{u}) = \phi_0(\underline{r}) + \underline{u} \cdot \nabla \phi_0(\underline{r}) + \cdots$$

$$+ (1 + k) V(\underline{r}) + \cdots$$

where $\cdots$ is $O(u_r^2)$

Now $\underline{u} \cdot \nabla \phi_0 = g u_r(\underline{r})$

$$= - h V(\underline{r})$$

Love number

Thus

$$\phi(\underline{r} + \underline{u}) = \phi_0(\underline{r}) + [1 + k - h] V(\underline{r})$$

this pot. on $r = a$ in absence of deformation

<u>Change</u> in potential on displaced surface thus:

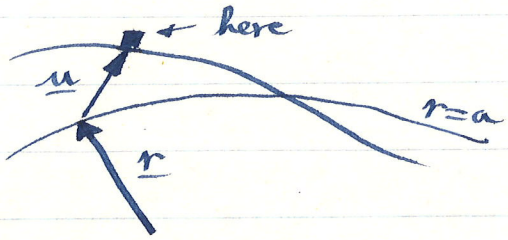

$$\delta\phi(\underline{r},t) = [1+k-h]\, V(\underline{r},t)$$

Grav. potentiometer would thus allow measurement of the combination $1+k-h$.

All other measurements on ⊕ surface can be expressed in terms of other combs. of Love nos. as we'll see in a moment. First, we note an interesting exploitation of above formula.

Kelvin and Darwin's determination of the rigidity of the ⊕:

The height of an equilibrium ocean tide on ⊕ acts as a sort of grav. potentiometer.

Tidal forces of ☾ and ☉ deform solid ⊕ and attract the oceans. If oceans respond in equilibrium they would conform to displaced equipotential

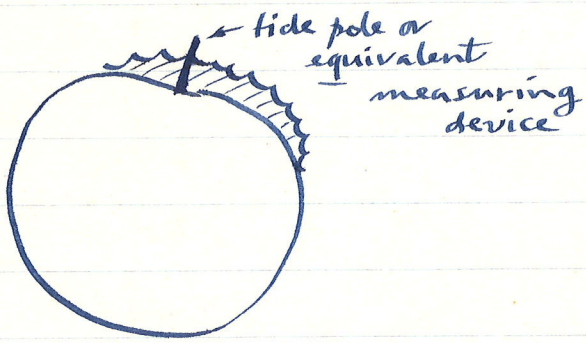

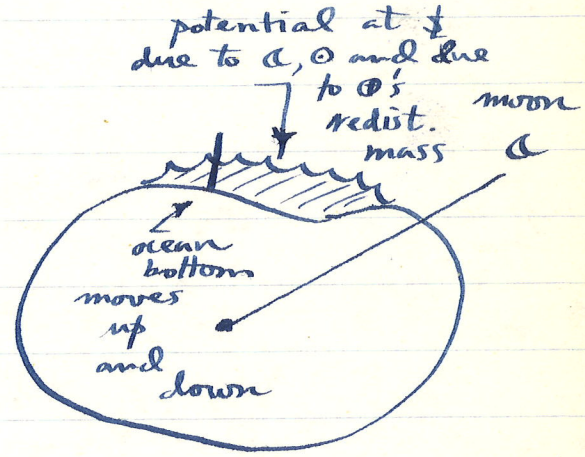

The equilibrium tide on an elastic ⊕ is displacement of equipot. surface relative to ocean bottom.

Easy to show that:

direct attraction of ☾, ☉ displaces equipot.

extra pot. due to redistr. ⊕ mass

$$\mathcal{G}(\theta,\phi,t) = -\frac{1}{g}\left[\underbrace{1+k}-h\right]V(\theta,\phi,t)$$

equilibrium tide

displacement relative to c.o.m. ⊕

but ocean bottom moves up

On rigid ⊕, $k = h = 0$ and $\mathcal{G} = -\frac{1}{g}V$ as before.

This idea led to first (<u>pre-seismology</u>) measurement of mean rigidity of ⊕ as a whole by Kelvin and Darwin in 1880's.

General idea: if ⊕ completely rigid then equil. tide $= -\frac{1}{g}V$. On a yielding ⊕ differs by factor of $1+k-h$. Kelvin first person to appreciate that tides would deform solid but elastic ⊕. Suggested could be employed to find $\bar{\mu}_{\oplus}$.

Background: accepted view of ⊕ at that time: <u>molten</u> interior, thin congealed crust

Reasons:

1. Temp ↗ as go down in mines. Simple extrapolation of $(dT/dz)_{surf}$ suggested molten below ~ 100 km. Now known that geothermal gradient decreases with depth.

2. volcanoes

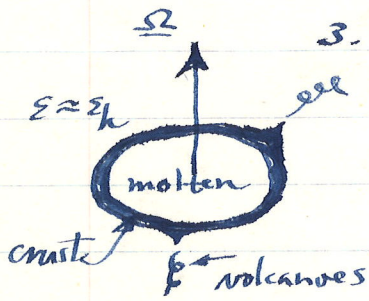

3. important to classical physicists like Kelvin who had read Principia, etc. : $\varepsilon \approx \varepsilon_{hydro}$ implies ⊕ fluid-like.

The diurnal and semi-diurnal tides are not equil. but Kelvin, following Laplace, reasoned that the fortnightly (Mf) tide would be very nearly so since 2 wks ≫ oceanic free periods.

Kelvin used elasticity theory to compute $1+k-h$ for a simple ⊕ model (actually he did not employ Love no. notation – introduced later)

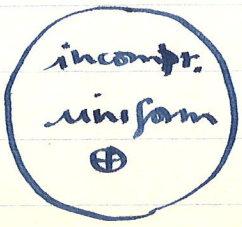

radius a
incompressible $\kappa(r) = \infty$
homogeneous $\mu(r) = \mu$, $\rho(r) = \rho$

<u>uniform</u> rigidity μ, density ρ

Result : g = gravity

$$\boxed{k = \frac{3/2}{1 + \frac{19}{2}\frac{\mu}{\rho g a}} \quad , \quad h = \frac{5/2}{1 + \frac{19}{2}\frac{\mu}{\rho g a}}}$$

Note for an incompr. <u>fluid</u> $\mu = 0$ and $k = 3/2$, $h = 5/2$.

Rigid ⊕ : $\mu = \infty$, $k, k = 0$.

For a fluid ⊕ : $1 + k - h = 1 + \frac{3}{2} - \frac{5}{2}$
$= 0$!

Makes sense : no ocean bottom, so ht. of tide <u>above</u> ocean bottom zero.

$$1 + k - h = 1 - \frac{1}{1 + \frac{19}{2}\frac{\mu}{\rho g a}}$$

In general :

$$\underset{\text{fluid } \oplus}{0} \leq 1 + k - h \leq \underset{\text{rigid } \oplus}{1}$$

Tide will be <u>reduced</u> on a yielding ⊕. If 19th cent. view of ⊕ correct Mf tide would be very small.

G.H. Darwin undertook analysis of available records : 14 Indian + British ports, 66 years total

Concluded that $1+k+h = 0.7 \pm 0.1$, a reduction of only 30%.

Not an easy measurement : Mf tides are only 1–2 cm in amplitude, C_j is 0.1564 and shape $\propto P_2(\cos\theta)$ which is near nodal at mid-latitudes.

$$\frac{1}{1+\frac{19}{2}\frac{\mu}{\rho g a}} = 0.3 \pm 0.1$$

Knowing $\rho = 5.5$ gm/cm^3, $g = 980$ cm/sec^2
$a = 6.371 \cdot 10^8$ cm gives

$$\boxed{\mu = \underset{\text{dyne cm}^{-2}}{8 \cdot 10^{11}} \sim \mu_{\text{steel}}}$$

A famous result "the ⊕ has the rigidity of steel". Very surprising at the time, now only of historical interest.

Seismology has provided us with a much more accurate picture of $\mu(r)$. S waves would not propagate in a fluid.

$\mu(r) = 0$ in fluid core but overall average for mantle very nearly μ_{steel}, a success for Kelvin to offset his determination of the ⊕'s age.

Recent studies of Mf tide at island tidal stations in Pacific show it to be nearly but not exactly "equilibrium" taking defm. of solid ⊕ into account.

If admittance defined by:

$$\text{admittance} = \frac{\text{measured amplitude}}{\text{theoretical quasi-static ampl. on yielding ⊕}}$$

then it varies from 0.7 to 1.2 about 20–30% and the phase varies w.r.t. equil. by ± 20°. Thesis by D. Luther MIT.

These variations due to propagation of

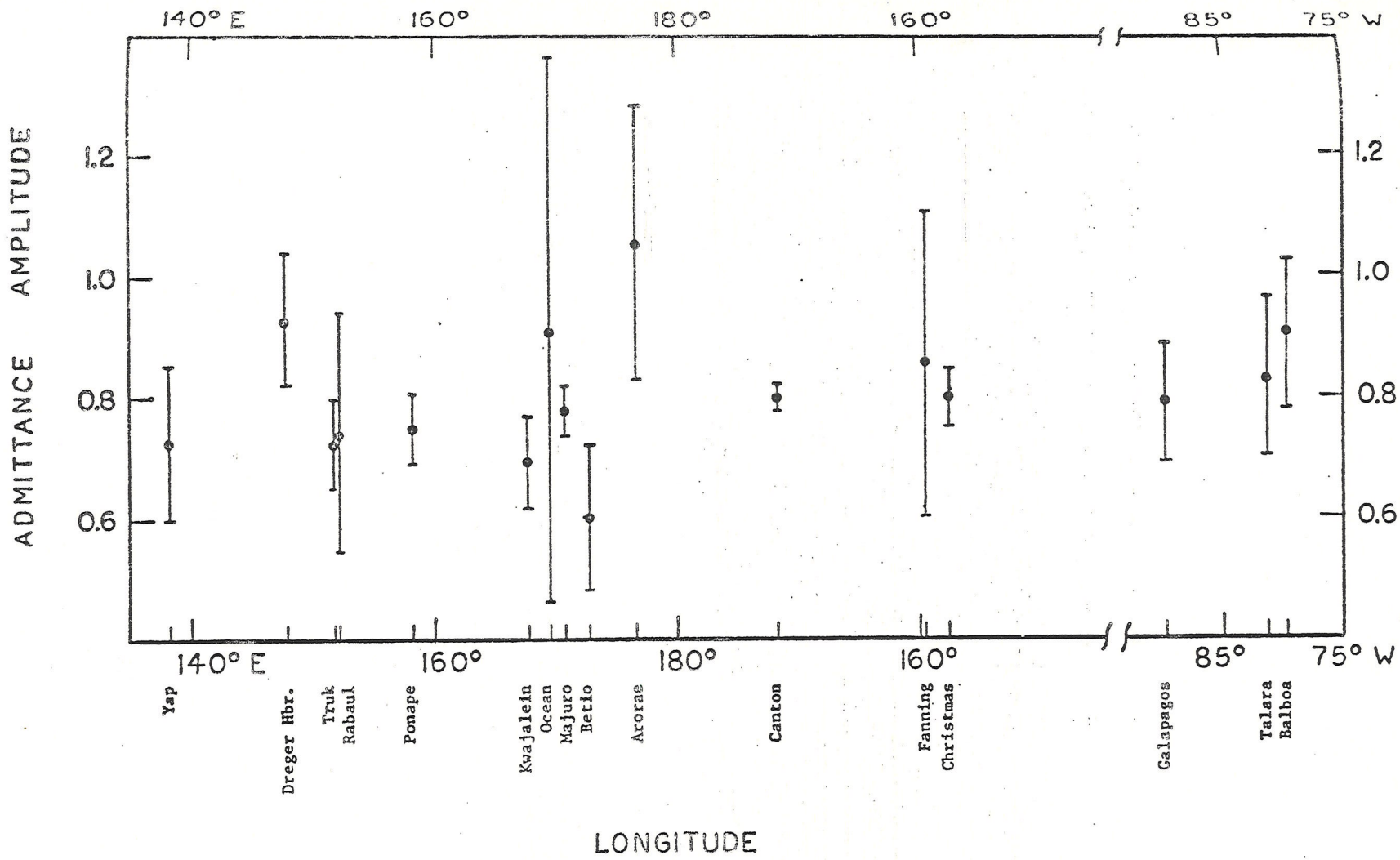

Figure 3.4a

Figure 3.4 - Admittance amplitude (a), and phase (b), of the fortnightly (Mf) tide plotted vs. longitude for all stations in the Pacific within 10° degrees of the equator and with more than one year of data. Exceptions are that Buenaventura and La Libertad are not plotted (see text). 95% error bars are indicated.

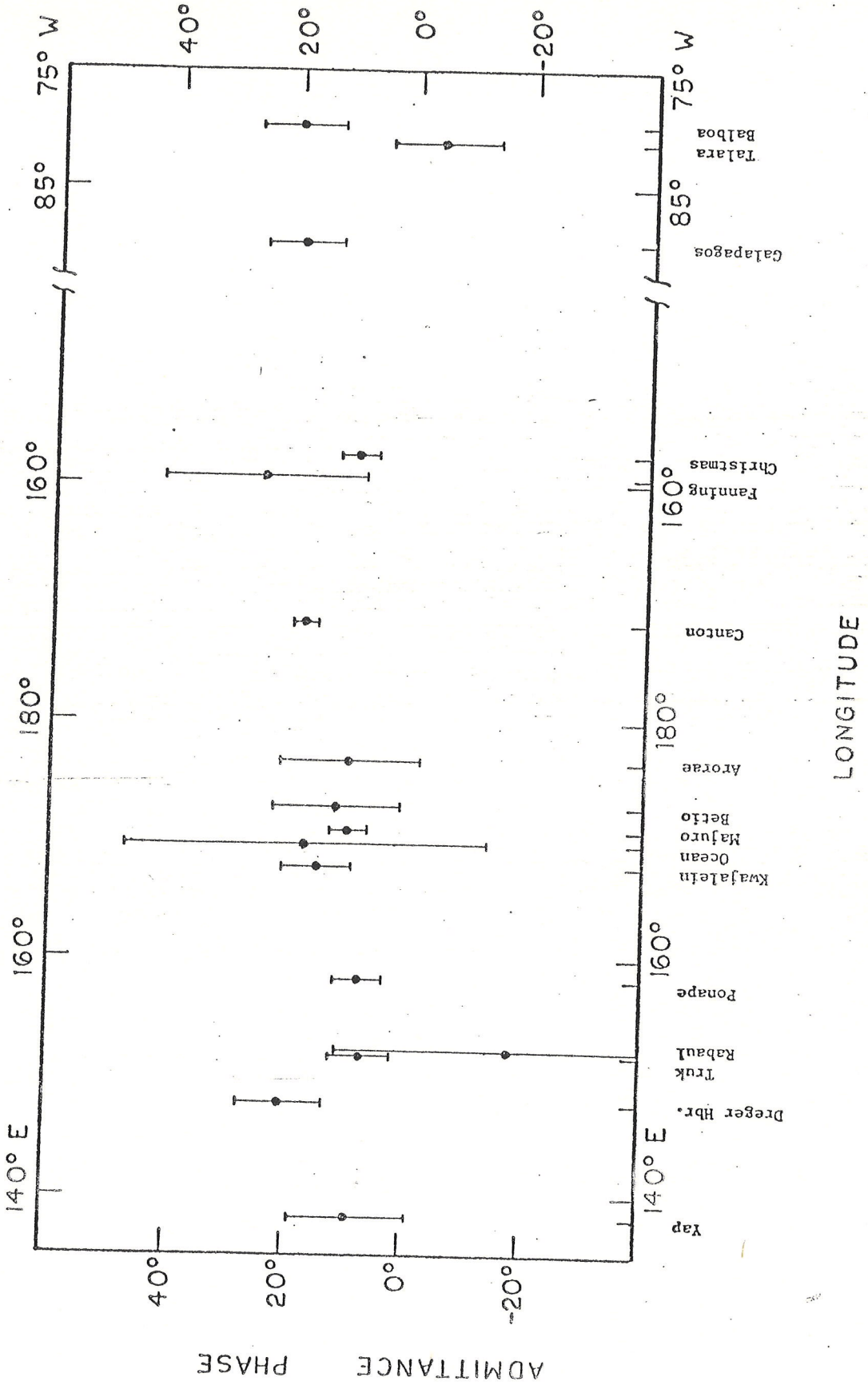
ADMITTANCE PHASE
40°
20°
0°
-20°
140° E
160°
180°
160°
75° W
85°
Yap
Dreger Hbr.
Truk
Rabaul
Ponape
Kwajalein
Ocean
Majuro
Betio
Arorae
Canton
Fanning
Christmas
Galapagos
Talara
Balboa
LONGITUDE

Figure 3.4b

so-called Rossby waves with speeds much slower than $c = (gH)^{1/2}$ for gravity waves, restoring force for Rossby waves is <u>Coriolis force</u>, a curious beast indeed, of great oceanographical interest.

Reason $\varepsilon \approx \varepsilon_{hydro}$ is that behavior of rocks at high temps. and on long time scales is <u>not elastic</u>.

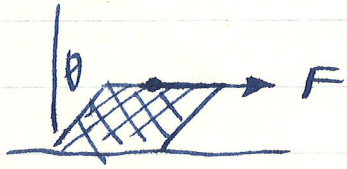

On short time scale (a few years or less) behavior is elastic and θ given by $F/A = 2\mu\theta$ elastic deformation.

On longer time scales even for small loads rock can <u>creep</u> due to motion (glide + climb) of dislocations in xtals, <u>rate</u> of creep measured by <u>viscosity</u> ν which as we have seen is $\sim 10^{21}$ to 10^{22} for mantle.

Actually, lab experiments on ~~[illegible]~~ olivine show its creep at high temps. actually governed by a <u>power</u> law relationship, not simple viscosity, $\dot{\varepsilon} \propto \tau^3$.

Tidal gravimetry and ocean loading

Best modern measurements of tides of solid ⊕ come from tidal gravimeters, measure changes in grav. acceleration on displaced outer surface

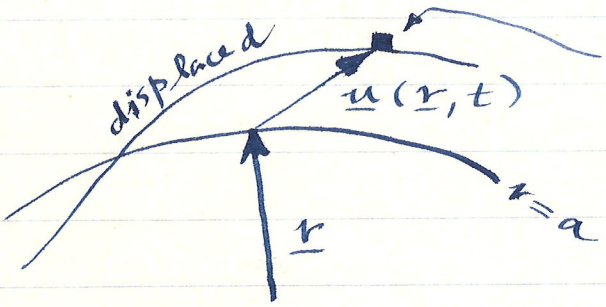

what is change in grav. acceleration $\equiv$ |grad potential| here on ⊕ surface?

Derivation slightly more long-winded than for change in potential itself.

Result:

$$\delta g(\underline{r},t) = \left[1 + h - \tfrac{3}{2}k\right]\frac{2}{a}V(\underline{r},t)$$

change in downward gravitational acceleration

direct attraction of ☾ or ☉

lifting of gravimeter further from c.o.m. (note − sign)

attraction of tidal bulge (note + sign)

when ☾ or ☉ overhead $V(\underline{r},t)$ is negative

$1+h-\frac{3}{2}k$ called the <u>gravimetric factor</u>. It is the combination of Love numbers which can in principle be ~~[illegible]~~ inferred from tidal gravity measurements.

For a modern ⊕ model

$$\boxed{1+h-\frac{3}{2}k = 1.159 \sim 1.16}$$

For many years the goal of ⊕ tide research was to measure $1+h-\frac{3}{2}k$ and other Love no. combs. (using other instruments) accurately: use to infer $\rho(r)$, $\kappa(r)$, $\mu(r)$ of ⊕.

This program largely unsuccessful. <u>Seismology</u> has given us a much better picture of $\rho(r)$, $\kappa(r)$, $\mu(r)$; can <u>compute</u> Love numbers for realistic ⊕ models more accurately than they can be measured.

Gravimeters calibrated to better than 1% but measurements

contaminated by <u>ocean loading effects</u>.

Can plot <u>expected</u> <u>gravity tide</u> in absence of oceans on a <u>phasor plot</u>.

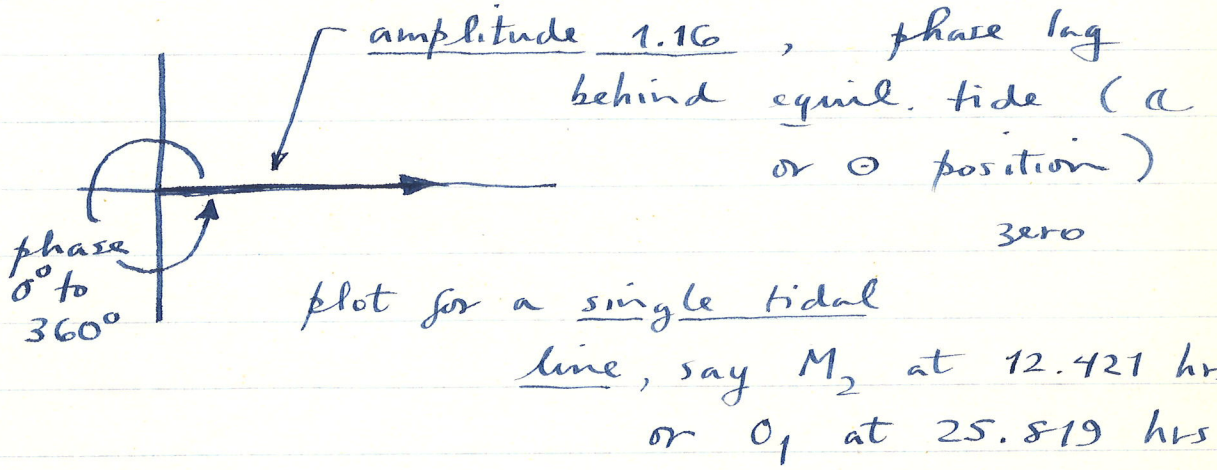

Typically measured $1 + h - \frac{3}{2}k$ ranges from 1.10 to 1.25 and phase $\pm$ 10° – 20°, i.e. deviations from theory of <u>order 10%</u>.

<u>Example</u>: superconducting gravimeter at La Jolla, Calif. and at Piñon Flat, Calif. (Goodkind et al.)

Fig. 1 power spectrum of gravity signal at La Jolla, see various tidal peaks indicated.

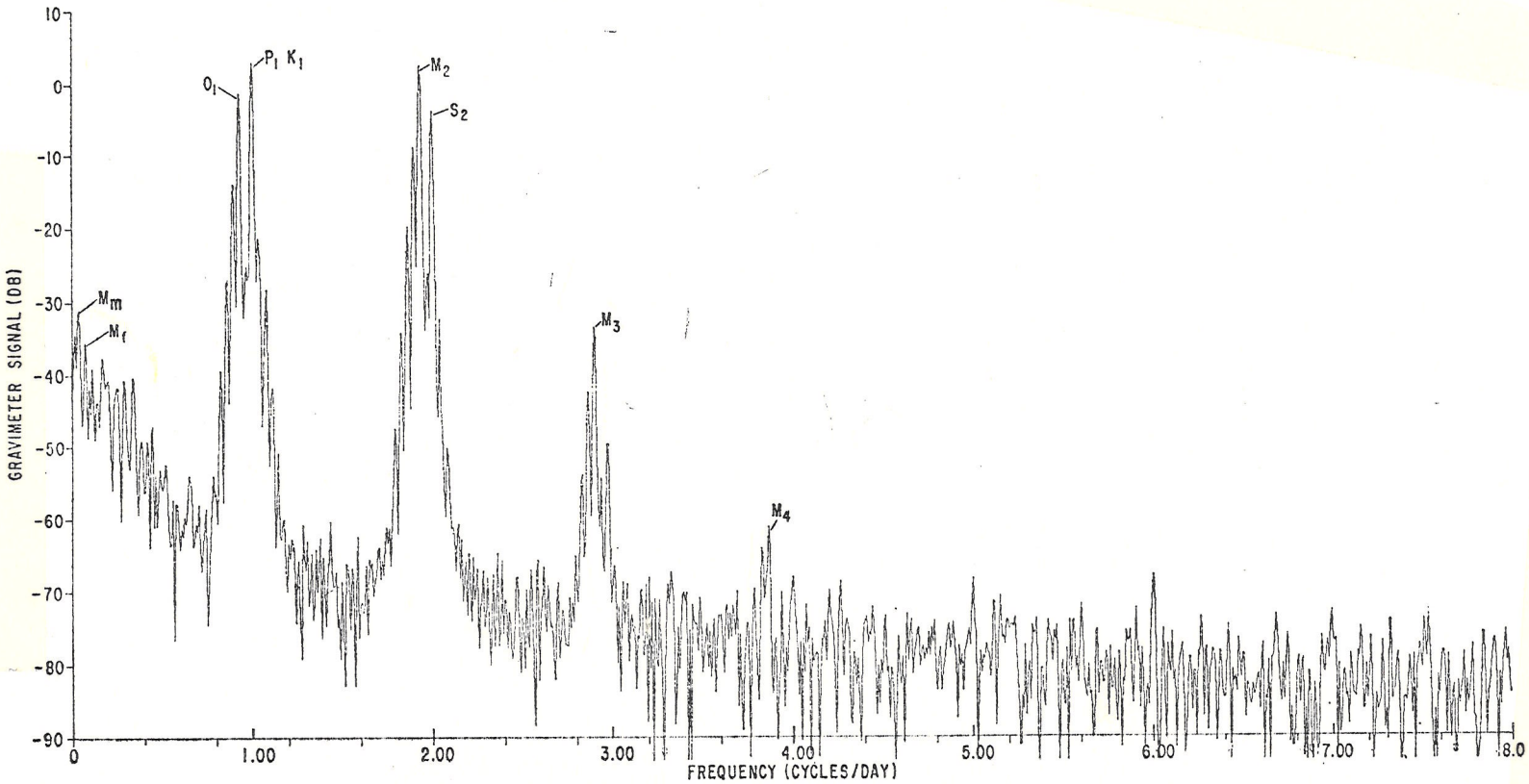

FIG. 1. Power spectrum of gravimeter signal for 100 days at La Jolla.

Note M_m and M_f, etc.
Note also M_3 etc. near 3 cpd
and M_4 etc. near 4 cpd.

These due to <u>neglected</u> terms in our development of $V(\underline{r}, t)$.
Recall we neglected terms of order

$$\frac{a}{R} = \frac{\text{radius of } \oplus}{\oplus \text{☾ distance}} \sim \frac{1}{60}$$

We expect M_3 down from M_2 by $1/60$, M_4 down $(1/60)^2$.
Amplitude scale is db, 6 db = factor of 2 so factor of 60 ~ 36 db ($2^6 = 64$). This checks.

Fig. 3 shows phasor plots for M_2 and O_1 at La Jolla and Piñon, blown up picture near end of arrow, data ●, ▲ etc. from different "runs" (need to fill Dewar to maintain liquid He temps several times during a "run").

M_2 lags equilibrium and O_1 leads it at both stations. Units 1 μgal $= 10^{-6}$ gal $\sim 10^{-9}$ g.

The discrepancy attributed to <u>ocean loading</u>.

<u>Three</u> effects on a gravimeter

1. direct attraction of H_2O <u>below</u> gravimeter
2. depression of ocean floor <u>lowers</u> gravimeter

these two largest both same sign.

3. load deforms solid ⊕

To correct for these effects need to know ocean tide everywhere, largest effect from nearby oceans, NE Pacific in this case.

we'll discuss these below.

Fig. 2 so-called <u>co-tidal charts</u> for M_2 and O_1 for this region, one of best known in world, many deep sea capsule drops by group at SIO.

The authors <u>integrated</u> effects of these ocean tides (NEP), added integrated

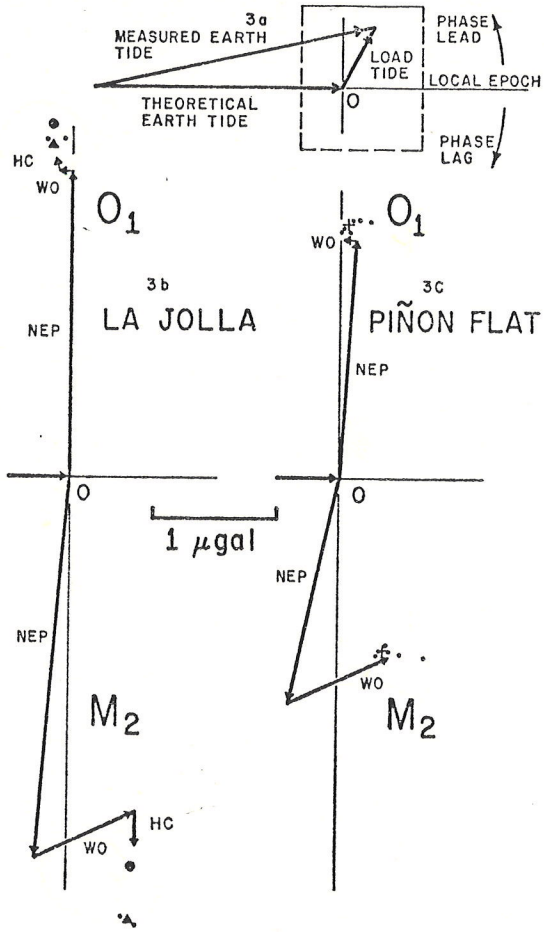

FIG. 3. Polar plots of ocean loading part of measured and theoretical O_1 and M_2 earth tide at La Jolla and Piñon Flat. The origin (O) is the end point of a vector representing the local theoretical tide of the solid earth with gravimetric factor 1·160 and zero phase lag. The load tide amplitude is represented by the distance from the origin to the observations (●, ▲, +, •) or to the tips of the theoretical load vectors. The phase lag is measured clockwise. At La Jolla ● is run 1, ▲ is run 2, and • are two 54-day sections of run 2. At Piñon Flat + is run 3 and • are six 54-day sections of run 3. The theoretical load vectors are calculated for the north-east Pacific Ocean (NEP) and for the 'rest of the world oceans' (WO) which is identical at the two locations. A correction for the height above the local ocean (HC) is made only at La Jolla.

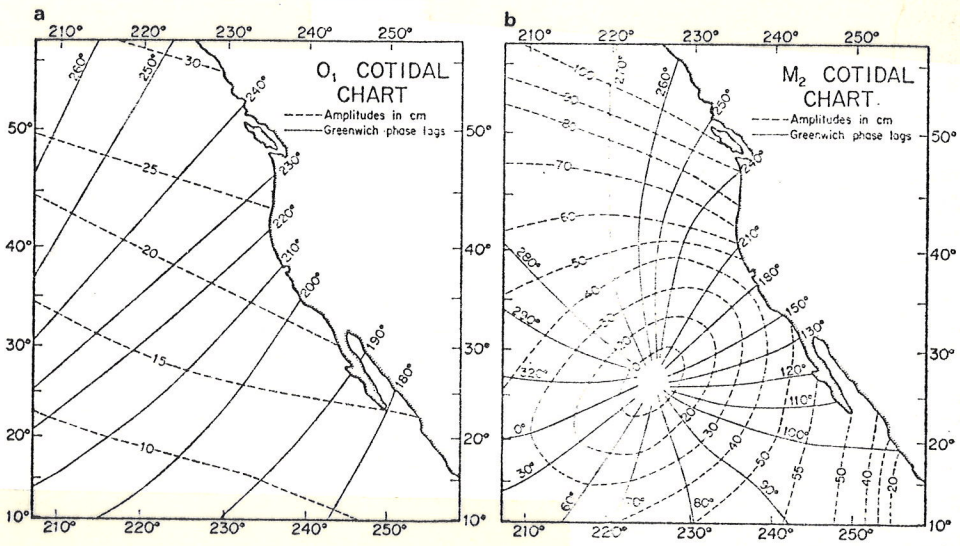

FIG. 2. (a) Modified co-tidal chart for O_1. (b) Modified co-tidal chart for M_2.

effects of rest of world's oceans (WO).

Found excellent agreement with observations, observed phase and amplitude to within 0.2 percent.

Piñon ~ 100 miles inland and loading effects are, as expected, smaller.

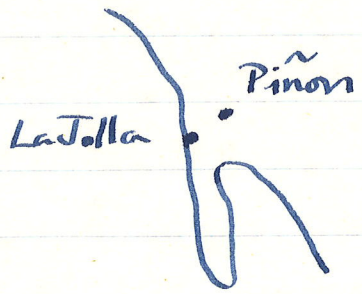

At both stations tidal loading effect of <u>order 10%</u>. Mid-continent measurements only affected by ~ 1%. This still too large to allow us to measure some things we would like, e.g. phase lag due to solid ⊕ anelasticity, which we expect to be of order .001° to .01° (Zschau) and fluid core resonance at <u>nearly diurnal free wobble</u> period.

Tidal <u>strain</u> measurements affected <u>much</u> more strongly by tidal loading, of <u>order 100%</u> at near coastal stations.

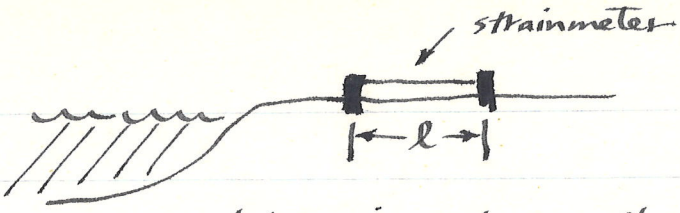

depression of seafloor
causes l to increase.

Also known now that these instruments severely affected by site geometry and local topography. These essentially act to concentrate + modify the global strain field.

There are people now attempting to turn ⊕ tide problem around : use grav. tide measurements on land to constrain deep-sea tides in poorly known areas. Each <u>load tide</u> measurement a weighted integral of deep-sea tides, leads to inverse problem.

Co-tidal charts and numerical models:

Recall the ocean tide for a single line can be written as:

tide as a fcn of θ, ϕ and t

$$h(\theta,\phi,t) = C(\theta,\phi)\cos(\sigma t - \Phi(\theta,\phi))$$

amplitude varies from place to place

tidal frequency different for different lines

phase varies from place to place

This conveniently represented by plotting in a so-called co-tidal chart.

Co-tidal lines are lines of constant phase $\Phi(\theta,\phi) = \text{const}$, typically in degrees from 0° to 360°, or in Greenwich hours from 0-12 for M_2 tide. Co-range lines are lines of constant amplitude in cm.

If the M_2 tide were equilibrium the co-tidal chart would look like

$$\bar{h} = 24.25 \sin^2\theta \cos(\sigma t - 2\phi)$$
cm.

Taking zero phase at <u>Greenwich</u>.

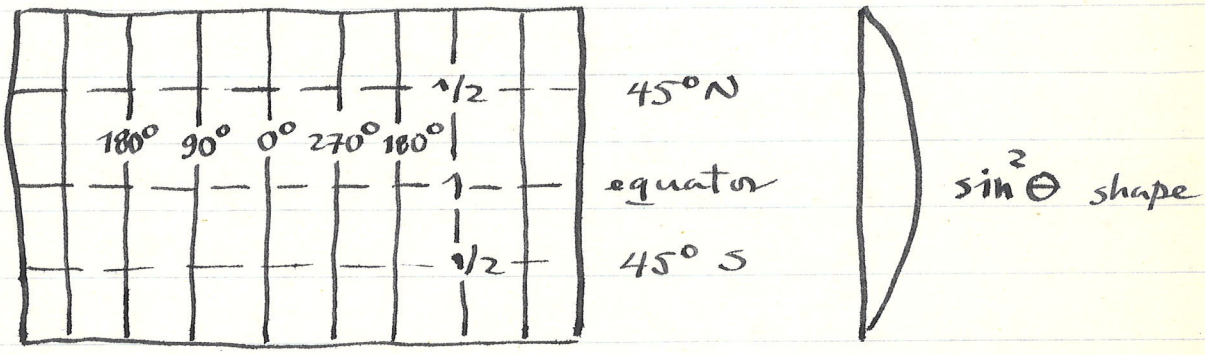

co-tidal lines are meridians
$\exists$ 2 high tides, if one on Greenwich then one on dateline.
co-range lines are lines of latitude.

Actual co-tidal charts for semi-diurnal and diurnal much more complicated. Originally constructed <u>empirically</u> by extrapolation from coastal and island observations.

In last few years several groups have succeeded in obtaining fairly realistic numerical solutions to

<u>Laplace's tidal equations</u>. PDE's which govern response of oceans to tidal input $\bar{h}$, corrected for yielding of solid ⊕ below oceans (Laplace assumed ⊕ rigid).

Equations depend on knowledge of <u>ocean depth</u> $H(\theta, \phi)$: must be prescribed numerically. Fig. 1 shows $H(\theta, \phi)$ smoothed, note e.g. <u>no</u> Mediterranean. LTE are <u>integro-differential</u> eqns in 3 coupled variables ζ = tide above ocean floor, u, v = N, E tangential velocity. See eqns (5)–(12) of Accad + Pekeris (1978).
Integro-part due to <u>tidal loading</u> and grav. <u>self-attraction</u>.
Solved numerically for M_2, S_2, O_1, a few others. <u>B.c. no flow into coasts.</u>

Principal feature of co-tidal charts is presence of <u>amphidromal</u> pts. or <u>amphidromes</u>, points where there is zero tidal variation

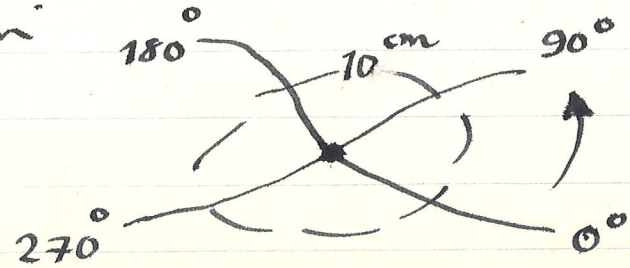

phase lines radiate out like spider legs

Tide progresses around amphidromes either clockwise or counter-clockwise. Phase must go from zero to 360° all the way around.

Fig. 9 shows Accad + Pekeris final solution for M_2 tide, note the dozen or so amphidromes, one in N. Atlantic, one in Pacific off coast of La Jolla, etc.

Note "anti-amphidrome" in Indian Ocean, whole basin goes up and down roughly simultaneously.

Fig. 10 shows comparison of phase and amplitude up Pacific Coast.

Fig. 9 shows agreement of theoretical amphidrome in Pacific with observations including several deep-sea capsule drop measurements by IGPP. Tide sweeps up California coast.

*

Amplitudes disagree 50°–60°N fjord effect

local amplification by confined bays.

Tide around <u>New Zealand</u> is interesting.

Tides are high ~ 100 cm a local maximum in S. Pacific, but phase goes around ccw <u>like</u> an amphidrome 180° out of phase on opposite sides of island.

Figs. 13 + 14 illustrate this in detail, note coarseness of <u>discretization</u>.

2. Modification of the tidal potential due to tidal self-attraction and to tidal loading

Let Ω denote the gravitational potential, defined so that the force F per unit mass is given by

$$F = -\operatorname{grad}\Omega. \tag{1}$$

With $\bar{\Omega}$ denoting the astronomical tidal potential, and $\bar{\zeta}$ denoting, in the standard notation (Lamb 1932, p. 332), the equilibrium tide, we have

$$\bar{\Omega} = -g\bar{\zeta}. \tag{2}$$

For the M_2 tide we have

$$\bar{\zeta} = 24.25\sin^2\theta e^{i(\sigma t+2\lambda)}\,\text{cm}, \tag{3}$$

where θ and λ denote colatitude and east longitude, and σ is the frequency of M_2. Let ζ denote the tidal elevation relative to the bottom. If ζ_s is the tidal elevation of the surface relative to the centre of the Earth, and ζ_b the tidal elevation of the bottom relative to the centre of the Earth, then

$$\zeta = \zeta_s - \zeta_b. \tag{4}$$

From this definition of ζ it follows that the equation of continuity retains the Laplacian form

$$\frac{\partial\zeta}{\partial t} = -\frac{1}{a\sin\theta}\left[\frac{\partial}{\partial\theta}(hu\sin\theta) + \frac{\partial}{\partial\lambda}(hv)\right], \tag{5}$$

where u and v denote the components of velocity (assumed uniform throughout the oceanic column), and $h(\theta,\lambda)$ is the variable depth of the ocean. In the presence of a bottom frictional force with components $F_{B\theta}$ and $F_{B\lambda}$, Laplace's tidal equations take the form

$$\frac{\partial u}{\partial t} - 2\omega v\cos\theta = -\frac{g}{a}\frac{\partial\zeta'}{\partial\theta} + \frac{1}{\rho h}F_{B\theta}, \tag{6}$$

$$\frac{\partial v}{\partial t} + 2\omega u\cos\theta = -\frac{g}{a\sin\theta}\frac{\partial\zeta'}{\partial\lambda} + \frac{1}{\rho h}F_{B\lambda}, \tag{7}$$

where ω is the speed of rotation of the Earth. In the original Laplace formulation (Lamb 1932, p. 332), ζ' stood for $(\zeta-\bar{\zeta})$, but this must now be modified to include (1) the effect of the elastic yielding of the Earth to the direct action of the astronomical tidal potential, (2) the effect of the elastic yielding of the Earth to the tidal loading, and (3) the self-attraction of the tides. If $-g\xi$ denotes the change in the gravitational potential due to effects (2) and (3), we have, by conventional theory,

$$\zeta' = \zeta - (1+k-h)\,\bar{\zeta} - \xi, \tag{8}$$

where k and h are Love numbers,

$$\xi(\theta,\lambda) = \alpha\sum_n \frac{\epsilon'_n\zeta_n}{(2n+1)} = \frac{\alpha}{4\pi}\int_0^{2\pi} d\lambda' \int_0^{\pi} \sin\theta'\, d\theta'\,\zeta(\theta',\lambda')\sum_n \epsilon'_n P_n(\cos\theta'), \tag{9}$$

$$\epsilon'_n = 1 + k'_n - h'_n, \tag{10}$$

$$\alpha = 3\rho/\bar{\rho} = 0.56, \tag{11}$$

and the axis of the coordinate system (θ',λ') passes through the point (θ,λ).

Here k'_n and h'_n denote loading Love numbers, $\bar{\rho}$ the mean density of the Earth ($= 5.57\ \text{g cm}^{-3}$), and ζ_n denotes the nth spherical harmonic component of the tide ζ:

$$\zeta = \sum_{n=1}^{\infty}\zeta_n. \tag{12}$$

In (12) we have omitted the term ζ_0, because it comes out to be only of the order of a millimetre for the two types of boundary conditions which we have used.

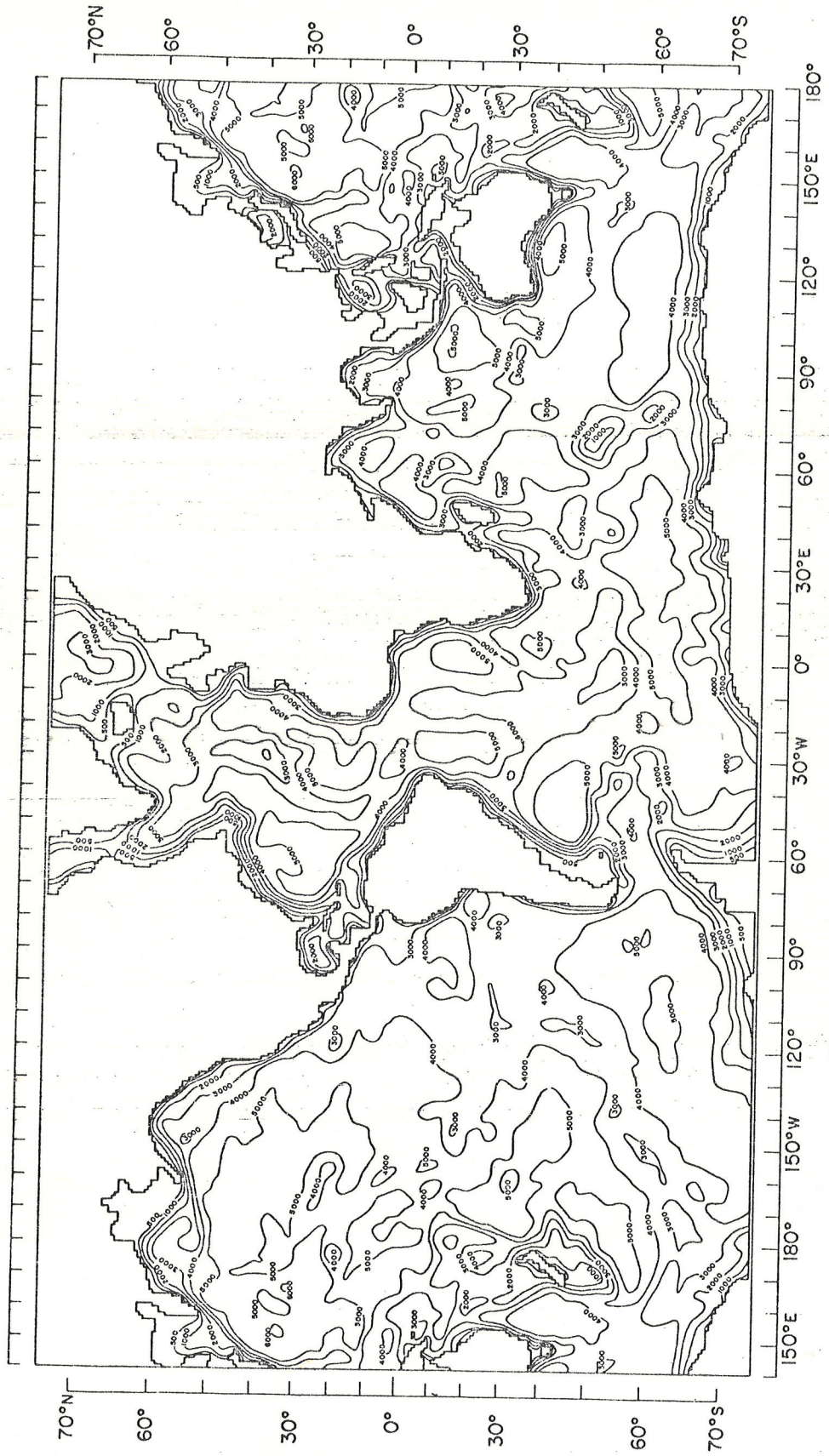

FIGURE 1. 1° map. Contour lines of depths of world oceans (in metres).

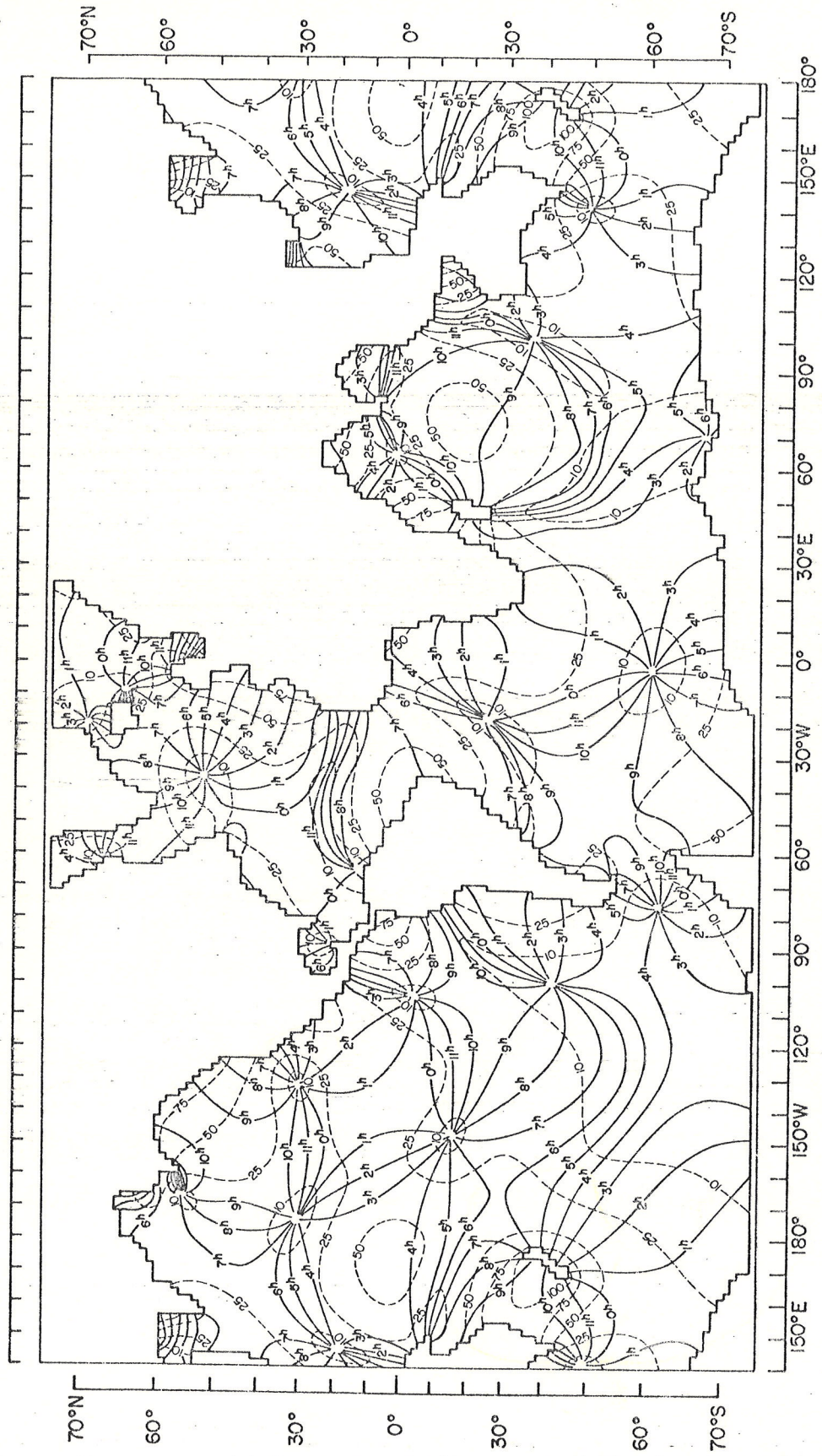

FIGURE 8. M_2 tide, including effects of self-attraction and of tidal loading. 2° grid, sloping shelf, $h' = 10$ m, $S = 100$ km. ——, Cotidal lines (Greenwich hours); - - -, corange lines (units: cm).

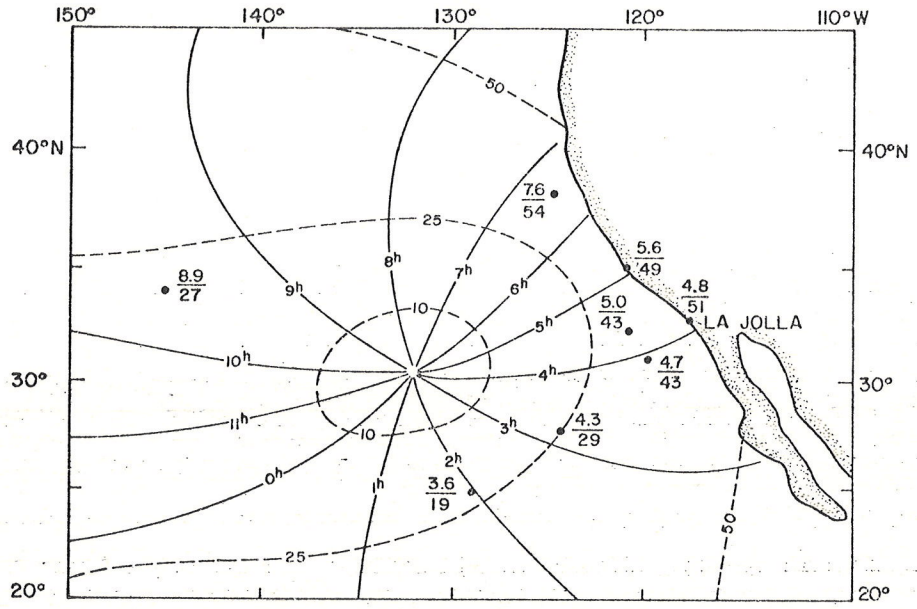

FIGURE 9. M_2 amphidrome in the northeast Pacific. Observed values (time/amplitude) taken from Irish *et al.* (1971).

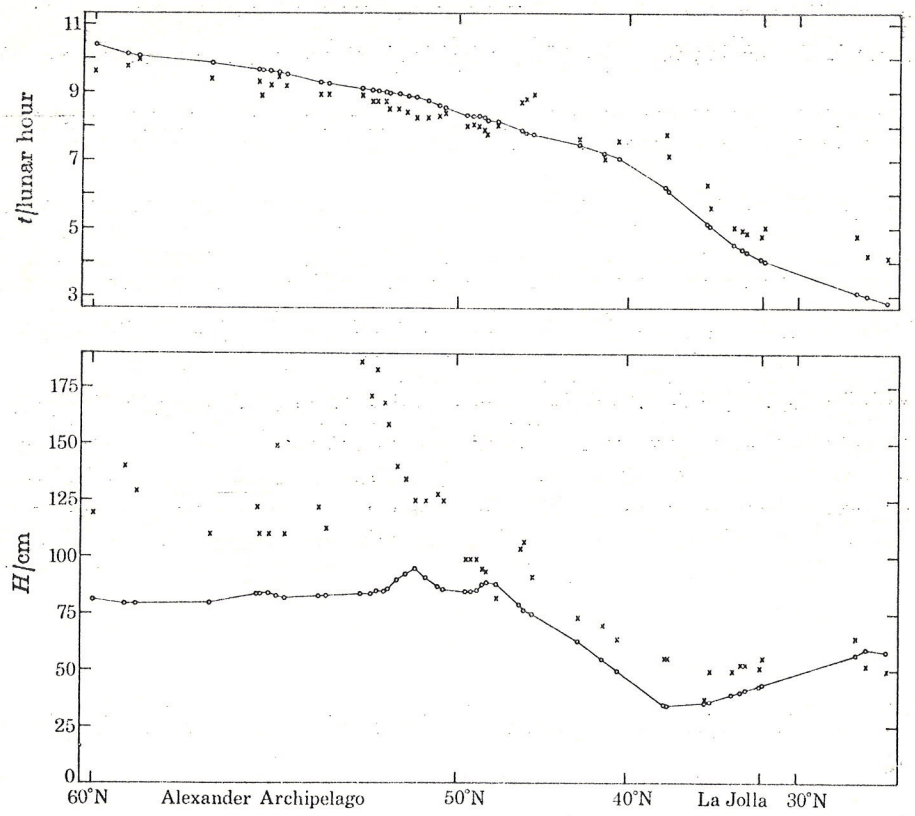

FIGURE 10. Comparison of observed with theoretical tides along the northeastern Pacific coast. ×, Observed; o, theoretical.

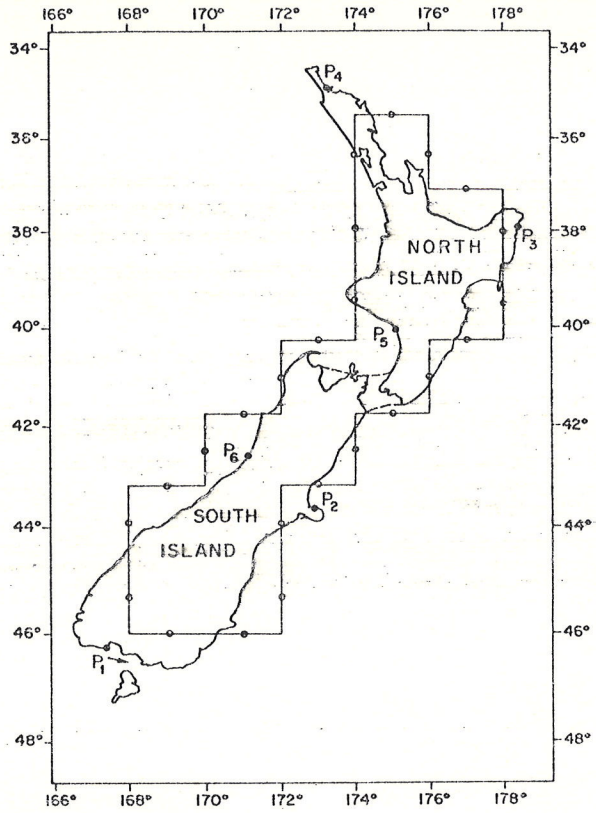

FIGURE 13. The New Zealand coast $P_1 \ldots P_6$, and the neighbouring grid-points.

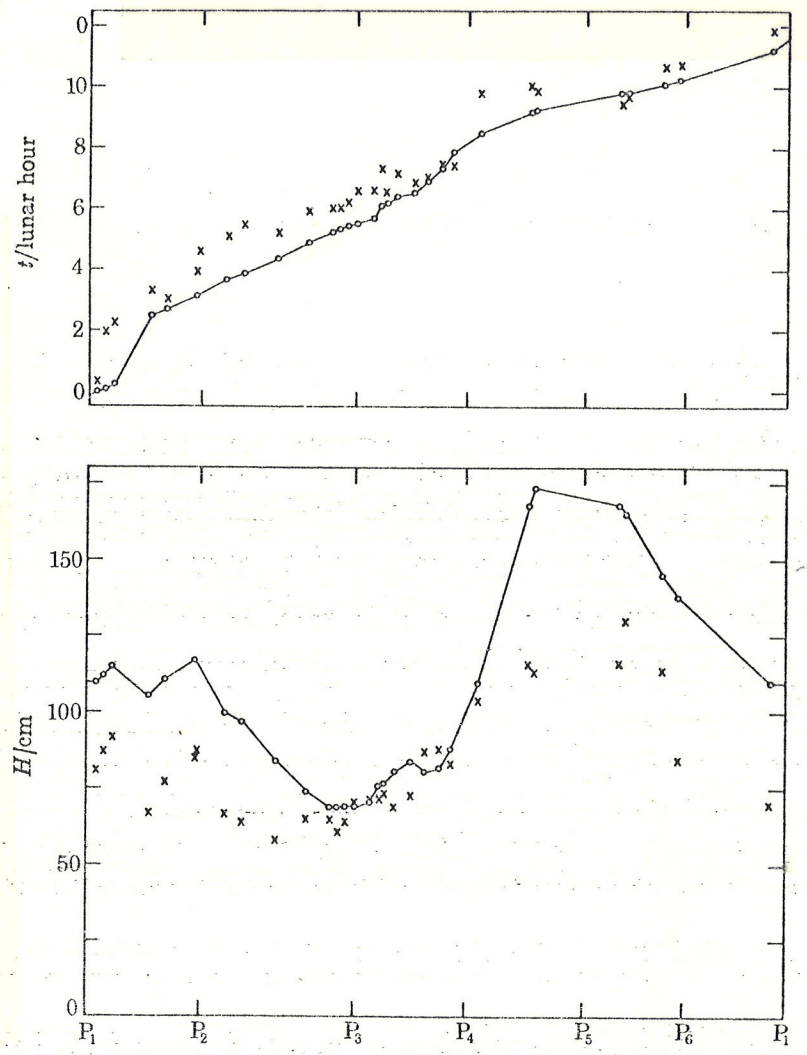

FIGURE 14. Comparison of observed wth theoretical tides on the New Zealand coast. ×, Observed; o, theoretical.